Global Anthropogenic Emissions (CAMS-GLOB-ANT) for the Copernicus Atmosphere Monitoring Service Simulations of Air Quality Forecasts and Reanalyses

Antonin Soulie[1], Claire Granier[1,2,3], Sabine Darras[4,7], Nicolas Zilbermann[4], Thierno Doumbia[1], Marc Guevara[5], Jukka-Pekka Jalkanen[6], Sekou Keita[1], Cathy Liousse[1], Monica Crippa[7,8], Diego Guizzardi[7], Rachel Hoesly[9], Steven J. Smith[9]

[1]Laboratoire d'Aérologie, Université de Toulouse, CNRS, UPS, Toulouse, France
[2]NOAA Chemical Sciences Laboratory, Boulder, Colorado, USA
[3]CIRES, University of Colorado Boulder, Boulder, Colorado, USA
[4]Observatoire Midi-Pyrénées, Toulouse, France
[5]Barcelona Supercomputing Center, Barcelona, Spain
[6]Department of Atmospheric Composition Research, Finnish Meteorological Institute, Helsinki, Finland
[7]Joint Research Center, Ispra, Italy
[8]Unisystem S.A., Milan, Italy
[9]Joint Global Change Research Institute, Pacific Northwest National Laboratory, College Park, MD, USA

Correspondence to: Antonin Soulie (Antonin.soulie@aero.obs-mip.fr)

Abstract.

Anthropogenic emissions are the result of many different economic sectors, related to transportation, power generation, industrial, residential and commercial activities, waste treatment and agricultural practices. Air quality models are used to forecast the atmospheric composition, analyse observations and reconstruct the chemical composition of the atmosphere during the previous decades. In order to drive these models, gridded emissions of all compounds need to be provided. This paper describes a new global inventory of emissions called CAMS-GLOB-ANT, developed as part of the Copernicus Atmosphere Monitoring Service (CAMS). The inventory provides monthly averages of the global emissions of 36 compounds, including the main air pollutants and greenhouse gases, at a spatial resolution of 0.1x0.1

degree in latitude and longitude, for 17 emission sectors. The methodology to generate the emissions for the 2000-2023 period is explained, and the datasets are analysed and compared with publicly available global and regional inventories for selected world regions. Depending on the species and regions, good agreements as well as significant differences are highlighted, which can be further explained through an analysis for different sectors as shown in the figures in the supplement.

1. Introduction

The design of mitigation policies for both pollutants and greenhouse gases, and a verification of the efficiency of these policies rely on chemistry-climate and chemistry-transport models. In order to provide accurate results, these models require a good knowledge of the emissions inventories of many atmospheric compounds. These inventories provide the necessary information to calculate the concentrations of atmospheric species emitted from natural and anthropogenic processes: these species can then be affected by chemical transformations and transport processes, and lead to the formation of other chemical species. An accurate knowledge of the spatial and temporal distribution of primary emissions is therefore essential to quantify the impact of surface emissions on the distribution of atmospheric pollutants and greenhouse gases.

During the past decades, many emission inventories have been developed at the global and regional scales, as detailed in Section 2 and in Granier et al. (2023). In general, surface emissions are calculated as the product of activity rates, emission factors and other factors depending on the type of source. Such data, for example activity rates, take a long time to collect, and the development of inventories is also a time-consuming effort. Therefore, most inventories do not provide emissions for the most recent years.

As part of Copernicus (https://www.copernicus.eu), the European Union's Earth observation program, the Copernicus Atmosphere Monitoring Service (CAMS: https://atmosphere.copernicus.eu, Peuch et al., 2022) delivers near-real-time analyses on a daily basis and forecasts of the atmospheric composition at

the global scale (Flemming et al., 2015). CAMS delivers as well a global reanalysis, which provides consistent multi-annual global datasets of atmospheric composition since the year 2003 (Innes et al., 2019). The forecasts and reanalysis provide three-dimensional fields of aerosols, gaseous chemical species and greenhouse gases. In order to provide these forecasts and reanalysis, the CAMS chemistry-transport models require up-to-date surface emissions.

None of the currently publicly available inventories such as the ones described in Section 2 and in Granier et al. (2023) provide the emissions required by the CAMS forecasts and reanalysis: either they cover a too short period for the reanalysis, or they don't provide emissions for the recent and current years, as required for global forecasts. Therefore, a new dataset called CAMS-GLOB-ANT has been developed during the past few years, which includes the emissions for air pollutants and greenhouse gases for real-time forecasts, at the spatial and temporal resolution required by the CAMS and other chemistry-climate models. This paper describes the existing datasets (Section 2) used in the methodology to develop CAMS-GLOB-ANT (Section 3), the comparison of the dataset with other inventories (Section 4) together with information on studies done using the CAMS-GLOB-ANT dataset. Section 5 includes information on how to get access to the dataset.

2. Datasets used in the development of CAMS-GLOB-ANT

The version of the CAMS-GLOB-ANT global anthropogenic emissions described in this paper is version 5, which is based on the Emissions Database for Global Atmospheric Research (EDGAR, version 5), the emissions provided by the Community Emissions Data System (CEDS, O'Rourke et al., 2021a) which are used for the extrapolation of the emissions to the most recent years, the temporal profiles from the CAMS-GLOB-TEMPO dataset and the ship emissions from the CAMS-GLOB-SHIP dataset. Each of these inventories is described in the following paragraphs.

2.1 EDGAR emissions

EDGAR, the Emissions Database for Global Atmospheric Research (https://edgar.jrc.ec.europa.eu/, last access July 2023), is developed at the Joint Research Center (JRC) in Italy. EDGAR provides emissions as national totals and gridmaps at 0.1 x 0.1degree resolution at the global level, with yearly and monthly averages. The emissions are calculated using a technology-based emission factor approach for the different countries, and for 27 different sectors: the list of the sectors included in EDGARv5 is shown in Table S1.

The methodology used for the EDGAR emissions is described in Crippa et al. (2018; 2021) and online at: https://edgar.jrc.ec.europa.eu/methodology. We have used here version 5 of EDGAR, which provides for the 1970-2015 period, gridded emissions for greenhouse gases (CO_2, CH_4 and N_2O) as well as for air pollutants, i.e. CO, NOx, NMVOCs, NH3, SO2, BC and OC. The national totals and gridded emissions for the different years and sectors are publicly available at: https://edgar.jrc.ec.europa.eu/dataset_ap50 (last access, July 2023).

The emissions for 25 speciated volatile organic compounds are also provided by EDGAR up to the year 2012 (https://edgar.jrc.ec.europa.eu/dataset_ap432_VOC_spec; last access July 2023), following the methodology described in Huang et al. (2017).

2.2 CEDS emissions

CEDS, the Community Emissions Data System (https://www.pnnl.gov/projects/ceds, last access: July 2023) is developed at the Joint Global Research Institute in Maryland, USA. CEDS emissions are developed within an open-source framework that produces annual emission estimates for research and analysis. The methodology used to derive the global emissions is detailed in Hoesly et al. (2018) and in McDuffie et al. (2020).

We have used the version of CEDS from O'Rourke et al. (2021a) which provides global emissions at a 0.5x0.5 degree on a monthly basis for the following species: SO_2, NO_x, BC, OC, NH_3, NMVOCs, CO, CO_2, CH_4, N_2O. This dataset is available at: https://doi.org/10.25584/PNNLDataHub/1779095 (last access, July 2023). The country emissions are given for 57 sectors from 1750 to 2019 (O'Rourke et al., 2021b) are available at: https://doi.org/10.5281/zenodo.4737769 (last access, July 2023). The sectors included in the CEDS emissions by country are given in Table S1.

2.3 CAMS-GLOB-SHIP emissions

For the ship emissions, we have used the CAMS-GLOB-SHIP, version 3.1, dataset. These emissions are generated by the Ship Traffic Emission Assessment Mode (STEAM3, Johansson, 2017), which uses global vessel activity from years 2014-2018, constructed from both terrestrial and satellite data from Automatic Identification System (AIS) transponders, where all vessels larger than 300 tons and all passenger ships report their position with a few second intervals. It should be noted that the coverage of inland shipping data may be poor, because the use and coverage of AIS in inland waterways is not yet mandatory.

The earlier years, 2000-2013, have been back casted based on 2016 activity data and using scaling factors taking into account for fleet size growth, the lower energy efficiency and smaller ship size in previous years: these factors take into account the lower. These scaling factors are applied separately for various shipping segments.

Disruptions, like the COVID19 pandemic are considered, because the underlying activity data is based on observed ship locations. Changes in environmental regulation of the shipping sector have been included at global and regional levels. These include the establishment of Emission Control Areas (ECAs) for SOx and NOx in the Baltic Sea, North Sea and North America as well as Chinese domestic ECAs and vessel type specific rules for ships operating in European seas, as defined by the International Maritime

Organization (https://www.imo.org/en/OurWork/Environment/Pages/Emission-Control-Areas-(ECAs)-designated-under-regulation-13-of-MARPOL-Annex-VI-(NOx-emission-control).aspx, last access December 2023). A global Sulphur cap (limit on the sulphur content in the fuel oil used on board ships) became effective in Jan 1st 2020, which decreased SO_x and PM emissions, but the ECAs regions, which implement those rules several years before 2020 were unaffected by the cap. The CAMS-GLOB-SHIP emissions are provided for several chemical compounds, such as CO_2, CO, NO_x, NMVOCs, BC, OC and SO_2.

2.4 CAMS-GLOB-TEMPO temporal profiles

The CAMS-GLOB-ANT monthly variability is implemented using monthly averaged profiles from the CAMS-GLOB-TEMPO dataset, described in Guevara et al. (2021): the monthly temporal profiles used in CAMS-GLOB-ANT are available on the ECCAD database (https://eccad.aeris-data.fr, last access December 2023). These temporal profiles consider the primary atmospheric pollutants, NO_x, SO_2, NMVOCs, NH_3, CO and the greenhouse gases CO_2 and CH_4, for the following sectors: energy, industry, road transportation, residential and agriculture (livestock, soil and agricultural waste burning), which have a direct correspondence with the sector classification considered in CAMS-GLOB-ANT (Table S1). For the sectors not considered in CAMS-GLOB-TEMPO, the EDGAR version 5 monthly profiles are used.

The temporal profiles are available at a 0.1x0.1degree spatial resolution. These temporal profiles are based on statistical information linked to emission variability at national and regional levels, such as electricity production statistics or measured traffic counts. Parameterizations accounting for meteorological conditions and sociodemographic factors are taken into account in the temporal profiles, including the use of a heating degree day approach. An example of the monthly temporal weights for the residential sector are shown for Madrid (Spain) and Capetown (South Africa) from 2000 to 2020 in Figure 1. The reported seasonality illustrates the role of meteorological conditions on the temporal variation of the residential emissions. For instance, the three largest peaks computed for Madrid in February 2015,

January 2017 and January 2019 coincides with the occurrence of three unusual cold spell and snowfall events that affected this region.

We have used the most recent version of CAMS-GLOB-TEMPO, i.e. version 3.1, which provides temporal profiles from 2000 to 2020. For all the years after 2020, the 2020 monthly temporal profiles have been used.

3. Methodology used for the development of CAMS-GLOB-ANT version 5

3.1 Definition of the sectors

CAMS-GLOB-ANT version 5 provides anthropogenic emissions for 17 sectors and for 35 species: CO_2 (divided into short organic cycle (released by combusting biofuels, agricultural waste burning or field burning) and excluding the short cycle), CH_4, N_2O, NO_x, NMVOCs, SO_2, BC, OC, NH_3 and 25 speciated volatile organic compounds. In order to calculate the emissions for the full 2000-2023 period for these sectors, a harmonization and grouping of the sectors of the EDGARv5 and CEDS datasets was performed. The sectors used in CAMS-GLOB-ANT are detailed in Table S1, and the corresponding sectors in the EDGARv5 and CEDS inventories are shown as well in this table. The sectors have been chosen, so that they represent the main anthropogenic activities corresponding to power generation, industrial activities, fuel operations, different modes of transportation, residential, agriculture activities and waste management. They have also been chosen, so that they are compatible with the definition of the sectors of the European dataset CAMS-REG (Kuenen et al., 2022). The sectors considered for the emissions of each of the 25 speciated volatile organic compounds considered in the inventory are indicated in Table S2.

3.2 Extrapolation of the emissions to the most recent years

In order to obtain emissions that can be used in global forecasts and long-term reanalyses, it is necessary to extrapolate the emissions to the most recent years and months. The EDGARv5 emissions are available until the year 2015 and the CEDS emissions are available up to 2019. We have used EDGARv5 emissions as a basis for the CAMS emissions, as their spatial resolution is 0.1x0.1 degree, which is the resolution of the emissions required by the CAMS global forecasts. The CEDS emissions are used for the extrapolation of the emissions up to the current year, i.e. 2023.

For this extrapolation, we have first grouped the CEDS emissions for each species, in order to obtain the totals emitted for each country for the sectors included in the CAMS-GLOB-ANT dataset, following Table S1. The relative change in the emissions for each country, species and sector for the 2013-2019, 2014-2019 and 2015-2019 period in the CEDS emissions was then calculated, as shown in Figure 2, which displays the results for three countries, the USA, Brazil and China for the emissions of nitrogen oxides. As shown by these figures, the changes in the emissions for the three considered periods are very close, and it was decided to use the 2014-2019 changes in the emissions for the extrapolation to the most recent years.

After grouping the CEDS emissions in order to match EDGARv5 sectors as shown in Table S1, we calculated a factor, called "growth factor" to quantify the change in the emissions, defined as:

$$q = \left(\frac{c_{tf}}{mean(c_{ti \to tf})}\right)^{\frac{1}{tf-ti}} \qquad (1)$$

where:

- q is the dimensionless growth factor

- c_{tf} is the emission for each country in 2019 (t_f) , and c_{ti} is the emission for each country for 2014 (t_i)

For three EDGARv5 sectors, there is no equivalent sector in the CEDS emissions: "non-ferrous metal production" (nfe), "agriculture waste burning" (awb) and "road transportation with resuspension" (tro_res). For the nfe and awb sectors, the growth factors are calculated on the basis of the 2013-2015 EDGARv5 values. For the sector "road transportation with resuspension" the same growth factor as for the road transportation sector is used.

An example of the growth factor for the industry sector for the SO_2 emissions is shown in Figure 3: this figure highlights the different patterns of recent changes in the emissions in the different countries of the world.

The emissions at a 0.1x0.1 degree resolution for each species and sector for the years after 2015 are then calculated following a geometric progression, by applying the growth factor as the common ratio for all the grid points in each country. Figure 4 presents in a schematic view of the methodology.

In EDGARv5, as indicated above, the emissions of speciated VOCs is available until 2012, from Huang et al. (2017). The extrapolation of the speciated VOCs is based on the calculation of the growth factor for the NMVOCs emissions from CEDS over the 2012-2019 period: an example of the growth factor for Germany is shown in Figure 5. This growth factor is applied to all the speciated VOCs provided by EDGARv5. As indicated above, the agricultural waste sector is not included in CEDS: for this sector, we have used the growth factor calculated over the 2013-2015 period for the NMVOCs species from EDGARv5.

3.3 Aircraft emissions

We have developed the aircraft emissions on the basis of the CEDS aircraft emission data described in Hoesly et al. (2018). For the years up to 2014, the emissions are taken from CEDS, which provides aircraft emissions for CO_2, CH_4, N_2O, CO, NMVOCs, BC, OC, NH_3 and SO_2. After 2014, a linear extrapolation using the trends calculated for the period 2012-2014 is applied to obtain the emissions for the most recent

years. The resulting dataset is CAMS-GLOB-AIR version 2.1, providing emissions from aircraft from 2000 to 2023, for 25 levels. The altitude of each of these levels is given in Table S3..

To be consistent with the VOCs speciation of the surface anthropogenic emissions, the emissions of speciated VOCs emissions from aircraft in CAMS-GLOB-AIR are based on the speciation described by Huang et al. (2017) for different emission sectors. We calculated the ratios of the emissions of each individual VOCs to the total NMVOCs species for each of these two altitude levels (landing/taking off and cruise altitudes) in the EDGAR dataset, at a 0.1x0.1degree horizontal resolution. The ratios for the landing/taking off level were then applied to the first two levels (0.305 km and 0.915 km) to the CAMS-GLOB-AIR NMVOCs species to get the aircraft emissions of each individual VOC. The ratios for the cruise altitude were applied to all the other levels indicated in Table S3 to obtain the emissions for the rest of the altitudes considered.

4. Results: The CAMS-GLOB-ANT version 5.3 emissions

The CAMS-GLOB-ANT version 5.3 emissions have been obtained using the methodology indicated in the previous sections, i.e. the extrapolation to 2023, the application of the CAMS-GLOB-TEMPO temporal profiles and the use of the CAMS-GLOB-SHIP emissions for ships. The results discussed in this paper will mainly focus on version 5.3 of the emissions.

It should be noted that the CAMS-GLOB-ANT version 5.3 emissions do not take into account the impact of the 2020 significant changes in emissions related to the lockdowns implemented by many countries to fight the COVID-19 pandemic. Another dataset, called CONFORM (COVID-19 adjustmeNt Factors fOR eMissions) described by Doumbia et al. (2021) provides adjustment factors at the same spatial resolution as the CAMS-GLOB-ANT emissions. The CONFORM adjustment factors are available for several sectors compatible with the CAMS-GLOB-ANT emissions. The CONFORM factors have not been implemented in the CAMS-GLOB-ANT dataset, in order to allow modelers to perform sensitivity studies, such as studies of the impact of the COVID-19 lockdowns on the global atmospheric composition.

The CAMS-GLOB-ANT_v5.3 inventory provides emissions as monthly averages, at a 0.1x0.1 degree in latitude and longitude spatial resolution. The spatial distribution of the yearly averaged emissions for CO, NO_x, NMVOCs, SO_2, BC and OC are shown in Figure 6. Relative changes in the annual global emissions since 2000 are shown in Figure 7: the relative change since the year 2000 is plotted for CO_2 (sum of CO_2_excluding_short_cycle and short_cycle), CH_4, CO, NO_x, NMVOCs, SO_2, BC, OC and NH3. For species such as CO_2, CH_4 and NH_3, a constant increase is seen for the past two decades. For the other species, a change in the trend (i.e. a decrease in the emissions) is shown around the years 2011-2014.

This feature is also shown in Table 1, which indicates the global totals emitted for the same compounds as in Figure 7 for 2000, 2003, 2009, 2012, 2015, 2018, 2021 and 2023 are indicated in Table 1, together with the trends from 2000 to 2012, and from 2012 to 2023. Even for the species for which a constant increase is seen, the trends after 2012 is significantly lower than before 2012. For CO, NO_x, SO_2, BC and OC, the emissions are decreasing after 2012, as a result of the implementation of several measures to limit the emissions of pollutants: these changes depend strongly on the regions and sectors, as discussed further in the following sections.

In order to better identify the reasons for the changes in the global total emissions from 2000, Tables S4 and S5 indicate the global totals emitted for several species and four groups of sectors for the years 2000, 2012 and 2023, as well as the 2000-2012 and 2012-2023 changes: Table S4 indicates the values for transportation (sum of road, non-road and ship transportation), and energy plus industrial activities (sum of the sectors power generation, refineries, industrial processes, fugitive and solvents), while Table S5 considers the emissions for the residential sector and agriculture/waste (livestock, soils, waste burning, and solid waste-waste water). For the global scale, these tables show that the decrease in the emissions or in the trends after 2012 are mostly due to changes in two sectors, transportation and energy + industrial activities. More details on the changes in the emissions for the different sectors will be given in the next section, which will focus of different world regions and countries.

5. Analysis of the CAMS-GLOB-ANT emissions and comparisons with other datasets

This section will analyze the changes in the emissions of CO, NO_x, NMVOCs, SO_2, NH_3, BC and OC for the regions for which regional inventories are available, i.e. Western Europe, Central Europe, the USA, China and India. The countries in each of the Western and Central Europe regions are indicated in Table S6. The changes in the total emissions for each of these regions from 2000 to 2012 and from 2012 to 2023 are shown in Figure 8. This figure shows significant differences between the trends in all species between the two periods.

These changes will be discussed in more details in the following sections. Comparisons will be performed using both regional inventories when available and the following global inventories: EDGAR version 5, EDGAR version 6 (published after the development of CAMS-GLOB-ANT version 5.3) and CEDS described in Section 2 and HTAP version 3 (Crippa et al., 2023 and https://edgar.jrc.ec.europa.eu/dataset_htap_v3, last access: July 2023). EDGAR and CEDS calculate the emissions on the basis of activity data and emission factors, while the HTAP dataset is based on a mosaic approach, and uses emissions reported by countries and regions when available. ECLIPSE version 6 (https://previous.iiasa.ac.at/web/home/research/researchPrograms/air/ECLIPSEv6b.html, last access: July 2023) is based on future scenarios after the year 2000. The older dataset called MACCity (Granier et al., 2011), based on a future scenario (RCP8.5, Riahi et al., 2011) after 2005 is also included in these comparisons as these emissions are used in the current CAMS reanalysis (Innes et al., 2019).

5.1 Western and Central Europe

As shown in Figure 8, the emissions of CO, NO_x, NMVOCs and SO_2, BC have decreased significantly in Western and Central Europe since 2000, while NH_3 and OC do not show a similar pattern. Tables 2 and 3 show the totals emitted for a few species for the same years as in Figure 8, and the corresponding percentage changes for Western Europe and Central Europe, respectively.

Large decreases in the emissions are found for the two 2000-2012 and 2012-2021 periods for all species, with the smallest changes for CO2, OC and NH_3 for both periods, and a slight increase in the NH_3 emissions in the past decade: for NH_3, the rather constant emissions during the full period are related to slight changes in the main contributor of these emissions, i.e. agriculture practices. Figure S1 shows, for Western Europe, the changes in the emissions for the different sectors considered for CO, NO_x, NMVOCs and SO_2, i.e. the species which show the largest changes.

For CO, the decrease in the emissions is mostly due to the implementation of strict rules in all European countries on the emissions from transportation: these emissions from transportation change from 28 Tg CO/year in 2000 to 2.9 Tg CO/year in 2023, with the largest change during the 2000-2012 period. Such changes have significantly modified the contribution of each sector to the total CO emissions in Western Europe, as shown in Figure 9: while the emissions from transportation represented 74% of the total emissions in 2000, they represent 21% of the total in 2023. The highest contribution to the emissions in 2023 is from the residential (43%) and industrial (26%) sectors.

The decrease in NO_x emissions is also mostly due to a decrease in the emissions from transportation, as shown in Figure S1, and to a lesser extent to the emissions from power generation: the contribution of the NO_x emissions from transportation decreased from 53% in 2000 to 41% in 2023, and the contribution of power generation decreased from 17% to 11% for the same period. At the same time, the contribution of industrial activities which remained rather constant, increased from 12 to 16%.

NMVOCs emissions have also decreased significantly, as shown in Table 2, mostly during the 2000s and early 2010s. This is mostly due to the decrease in the emissions of transportation: but, as the emissions from the solvents sector did not decrease, the NMVOCs emissions decreased only by 3% during the past decade.

SO_2 emissions from power plants, which were still rather important in 2000 have been strongly regulated and have decreased from 2.5 T SO_2/yr to 0.8 Tg SO_2/yr in 2023. However, the emissions of SO_2 from industrial activities, the 2nd largest contributor to the SO_2 emissions have decreased by about 30% of the full period, which explains the decrease in the emissions reported in Table 1.

Figure 10 shows a comparison of the CAMS-GLOB-ANT_v5.3 emissions with other inventories, i.e. the global inventories indicated at the beginning of Section 5, as well as with version 5.1 of the regional CAMS-REG dataset (Kuenen et al., 2022). For CO, all the inventories show similar values after 2009, except for MACCity and ECLIPSE, which show lower emissions after 2010: these two inventories are based on older scenarios after 2000-2005. For NO_x, the trends are similar among the inventories, with downward trends for the whole period. MACCity and ECLIPSE, based on scenarios, provide higher NO_x emissions in the most recent years. CAMS-GLOB-ANT and CAMS-REG show rather similar values: these two datasets use very different methodologies, CAMS-REG being based on values reported by countries at the EMEP organization (Wankmüller, 2019), while CAMS-GLOB-ANT is based on EDGARv5 and CEDS. For SO_2, the CAMS-GLOB-ANT emissions, which follow the EDGARv5 and the trends in the CEDS emissions are higher than the regional emissions at the end of the period, and slightly lower at the beginning of the period.

Rather similar patterns are seen in the change in the emissions of pollutants and greenhouse gases in Central Europe (Table 3 and Figure S2), with decreases in somewhat lower magnitudes, related to smaller changes in transportation emissions. The emissions of BC and OC have increased during the first considered period, mostly due to an increase in residential combustion and to road transportation to a lesser extent.

Plots of the comparisons of the emissions for Central Europe with global inventories and the regional CAMS-REG_v5.1 inventory are shown in Figure S3. The results of the comparison are similar to the comparisons for Western Europe: a larger spread of the values for the NMVOCs emissions can be noticed,

which could be related to the use of different average emission factors for these compounds, which represents the emissions of a lumping of different species.

5.2 United States of America

Changes in the US emissions of several species for the same years as considered in Table 1 are given in Table 4. The emissions of all species have decreased significantly, except for CH_4 and NH_3. The stability in the CH_4 emissions is related to constant oil and gas operations, as well as from livestock agriculture practices (fugitive and manure/enteric fermentation emissions in the EDGAR emissions). For NH_3, the constant increase is due to the use of fertilizers and livestock operations.

The changes in the emissions for the different sectors from 2000 to 2023 are shown in Figure S4, for CO, NO_x, NMVOCs and SO_2. The large decrease in CO emissions is mostly due to the decrease in the emissions from transportation, with the implementation of national standards for tailpipe emissions, new fuel programs and improvement in vehicle technologies: these standards are described in details in the website of the US EPA (Environmental Protection Agency, https://www.epa.gov/air-emissions-inventories, last access: December 2023). NO_x emissions have decreased importantly until the early 2010s, but a slowdown in the emissions reduction is seen after 2012, which consistent with the study of Jiang et al. (2018) based on satellite and ground-based observations. This slowdown can be explained by a growing contribution of off-road and diesel vehicles transportation emissions and industrial activities. The large decrease in SO_2 emissions is mostly due to the strict control in the emissions from power plants.

Comparisons were performed with the global datasets, together with the officially reported emissions by the EPA. The air pollution emissions trends data from 1970 to 2021 provided by EPA at https://www.epa.gov/air-emissions-inventories/air-pollutant-emissions-trends-data (last access: July 2023) were used. A rather good agreement is seen for the CO and NO_x emissions in the USA, except for the EDGARv6 emissions of CO, which are significantly lower: this is due to the use of smaller emission factors for road transportation and lower small scale combustion of biofuels in the EDGAR6 dataset.

The differences shown in Figure 11 between the inventories are larger for the NMVOCs species, particularly in the early 2010s, with larger emissions from the EPA dataset and the lowest values in the old MACCity emissions and in EDGAR6. These differences are related to the road transportation sector and to a lesser extent to the solvents sector.

380

5.3 China

Table 5, which shows the changes in the emissions of several species for the same years as considered in the previous tables reflects the measures taken as part of the Chinese Air Pollution Prevention and Control
385 Action Plan established by the Chinese Government in the early 2010s. From 2000 to 2012, the emissions of all species (except NH3) increased by 20% to 50% for most pollutants, and even 90% for NO_x. After 2012, only the emissions of CO_2 continued to increase, as well as the emissions of NMVOCs and NH_3 but with a low percentage.

The changes in the emissions for the different sectors from 2000 to 2023 are shown in Figure S5 for CO,
390 NO_x, NMVOCs and SO_2. The largest decreases after 2012 are for SO_2, for which the emissions from power generation and industrial processes decreased by 64% and 47%, respectively. NO_x emissions decreased as well, due to a 35% and 9% reduction in the emissions from power generation and industrial activities, respectively and a minor reduction in the emissions from transportation. For CO, the main reductions from 2012 to 2023 are seen in the sectors of transportation (-24%), residential (-20%) and
395 industrial activities (-11%). The NMVOVCs emissions have started to decrease slightly in 2015, as a result of a decrease in the emissions from transportation and from industrial processes. However, the emissions from solvents increased by 14% between 2012 and 2023.

Comparisons were performed with the global datasets, as well as with two regional inventories for China:
400 the REAS (Regional Emission inventory in Asia) version 3 published by Kurokawa and Ohara (2020) were used, downloaded from the REAS website (https://www.nies.go.jp/REAS/, last access July 2023), as well as the MEIC (Multi-resolution Emission Inventory model for Climate and air pollution research:

meicmodel.org.cn, last access July, 2023; Li et al., 2017; Zheng et al., 2018). REAS and MEIC provide emissions for a large number of species (except for CH_4) for 1950-2015 (REASv3) and 2008-2017 (version 1.3) for MEIC, respectively.

Figure 12 shows the differences between these inventories for CO, NO_x, NMVOCs and SO_2. For CO, large differences exist at the beginning of the 2000s, but the total emissions for China are closer at the end of the period. The large differences are mostly due to different estimates of the emissions from transportation between the global inventories, more particularly CEDS and EDGAR. It should be noted that the two regional inventories, MEIC and REASv3 show CO emissions closer to the EDGAR emissions in the 2000s and closer than the CEDS emissions in the mid-2010s.

NO_x emissions show similar patterns among the global and regional datasets, except for MACCity, which was developed before the Chinese plans for emissions reductions (Zheng et al., 2018; Kurokawa and Ohara, 2020). In 2018, the NO_x emissions from all the inventories are within 15% of each other. NMVOCs emissions agree rather well in the 2010s, except for the old MACCity dataset and the ECLIPSEv6 inventory, which is also based on future scenarios. For SO2, the agreement is rather good at the beginning of the 2000s, but the trends in the emission differ after 2013-2014: the EDGAR v5 and v6 emissions show smaller trends than the other datasets. The emissions provided by CAMS-GLOB-ANT_v5.3 first follow the EDGAR emissions: as the recent trends are based on CEDS, the trend in the CAMS emissions is closer to the trend shown by the regional emissions. As a result, the values of the CAMS-GLOB-ANT SO_2 emission in 2015-2019 are between the EDGAR and the emissions provided by the other datasets.

5.4 India

Table 6 shows the changes in the emissions of several species for the same years as considered in the previous tables. This table shows the large increases in the emissions of all species in this country from 2000 to 2012. After that date, some measures have started to be been taken to start reducing intense

pollution events, as part of the Indian National Clean Air Programme (Ganguly et al., 2020). Most emissions have continued to increase but at a slower rate than before 2012.

Figure S6 shows the changes in the CAMS-GLOB-ANT_v5.3 emissions of CO, NO_x, NMVOCs and SO_2 for the 2000-2023 period in India for the different sectors.

For all species, the emissions from the residential sector were almost constant during the considered period. The CO emissions peaked in 2015, and decrease afterwards as a result of the implementation of measures in the transportation and industrial sectors (Joshi et al., 2023). The NO_x emissions peaked as well in 2015, and stayed rather constant afterwards: this explains the slight increase in the emissions from 2012, driven by an increase in the emissions from transportation. Emissions of NMVOCs have continued to increase, mostly because of a constant increase of about 33% of the emissions from solvents. The moderate increase after 2012 is related to a decrease in the emissions from traffic of about 16% from 2015 to 2023.

SO_2 emissions are driven by the emissions related to power generation and industries, which have more than doubled between 2000 and 2014, followed by rather constant emissions. For BC, emissions from industrial activities and the residential sector represent 40% and 36% of the emissions, respectively. The emissions from the industrial sector decreased by about 20% from 2014 to 2023, which explains the slight decrease of the BC emissions during the 2012-2023 period.

Figure 13 shows a comparison of the emissions of CO, NO_x, NMVOCs and SO_2 with the global inventories mentioned in the previous sections and with the REASv3 regional inventory for Asia. The MACCity emissions, based on an old dataset (Granier et al., 2011) and the RCP8.5 scenario (Riahi et al., 2011) provides very different emissions than the other datasets. The other inventories are generally in a good agreement, though the recent trends in the CAMS-GLOB-ANT emissions can differ significantly: for example, the NO_x emissions are rather constant after 2015, while they increase in the ECLIPSE dataset (based on a future scenario). For NMVOCs, the CAMS-GLOB-ANT emissions are rather stable after 2015, which is consistent with the HTAPv3 and EDGARv6: however, in 2015, CAMS-GLOB-ANT emissions are about 15% lower than the HTAPv3 emissions and 20% higher than the EDGARv6

emissions. For SO_2, the CAMS-GLOB-ANT emissions are in good agreement with the HTAPv3, EDGARv5 and EDGARv6 emissions, and significantly higher than the CEDS emissions. For all species, the CAMS-GLOB-ANT emissions are globally in agreement with the REAS regional inventory.

More evaluation of the CAMS-GLOB-ANT emissions are given in modeling studies that have used the CAMS models or other models such as MUSICA (Multi-Scale Infrastructure for Chemistry Modeling: Tang et al., 2023), CESM (Community Earth System Model: Gaubert et al., 2021, 2023; Bouarar et al., 2021; Ortega et al., 2023).

6. Availability of the data

The gridded maps (CAMS-GLOB-ANT_v5.3) as monthly means data described in this manuscript can be accessed as NetCDF (Network Common Data Format) files at https://doi.org/10.24380/eets-qd81 (Soulie et al., 2023). They can also be accessed through the Emissions of atmospheric Compounds and Compilation of Ancillary Data (ECCAD) system at https://permalink.aeris-data.fr/CAMS-GLOB-ANT and with a login account (https://eccad.aeris-data.fr/, last access: July 2023). For review purposes, ECCAD has set up an anonymous repository where subsets of CAMS-GLOB-ANT_v5.3 data can be accessed directly (Soulie et al., 2023; https://eccad.aeris-data.fr/essd-surf-emis-cams-ant/, last access: July 2023).

7. Conclusions

The paper describes version 5 of CAMS-GLOB-ANT, a new inventory publicly available for global air quality and climate forecasts and reanalyses. The emission dataset is based on different datasets, i.e. the global inventories EDGAR and CEDS, as well as on temporal profiles from the CAMS-GLOB-TEMPO, ship emissions from CAMS-GLOB-SHIP datasets. A dataset called CAMS-GLOB-AIR provides also 3-dimensional emissions from aircraft exhaust. The CAMS-GLOB-ANT inventory was developed under the Copernicus Atmosphere Monitoring Service project (CAMS-81: global and regional emissions) as part of the European Union's Copernicus Earth Observation Programme.

CAMS-GLOB-ANT includes the emissions of 36 species, including the greenhouse gases CO_2 (excluding short cycle and short organic cycle), CH_4 and N_2O, atmospheric pollutants (CO, NO_x, NMVOCs, SO_2, BC, OC, NH_3 plus 25 speciated volatile organic compounds). The spatial resolution of the gridded emissions is 0.1x0.1 degree in latitude and longitude, and the temporal resolution is monthly.

The paper discussed the changes in the emissions for the main greenhouse gases and air pollutants, with a focus on CO, NO_x, NMVOCs and SO_2. Comparisons are made with the other global inventories publicly available and with regional emissions datasets available for Europe, the USA, China and India.

It should be noted that updated versions of the CAMS-GLOB-ANT dataset will be developed during the coming years. The current limitations of the inventory will be considered, such as the constant NMVOCs speciation after 2012 (following the EDGAR VOCs speciation), the inclusion of more up-to-date data for the extrapolations to the more recent years, the inclusion of the CONFORM adjustment factors for the COVID-19 lockdowns directly into the emission dataset and when possible the inclusion of regional information for the different species and sectors.

8. Author contributions

AS and CG developed the dataset and created the emission inventories. SD and NZ performed the emission data formatting and the upload to the database. TD, SK and CL participated in the analysis of

the emissions. MG and JPJ provided the CAMS-GLOB-TEMPO and CAMS-GLOB-SHIP datasets. MC and DG provided the EDGAR emissions and RH and SS gave access to the gridded CEDS data.

9. Competing Interests

The contact author has declared that none of the authors has any competing interests.

10. Acknowledgments

The development of the CAMS-GLOB-ANT dataset has been funded by the Copernicus Atmosphere Monitoring Service (CAMS), which is implemented by the European Centre for Medium-Range Weather Forecasts (ECMWF) on behalf of the European Commission.

References

Crippa, M., Guizzardi, D., Muntean, M., Schaaf, E., Dentener, F., van Aardenne, J. A., Monni, S., Doering, U., Olivier, J. G. J., Pagliari, V., and Janssens-Maenhout, G.: Gridded emissions of air pollutants for the period 1970–2012 within EDGAR v4.3.2, Earth Syst. Sci. Data, 10, 1987–2013, doi:10.5194/essd-10-1987-2018, 2018.

Crippa, M., Guizzardi, D., Pisoni, E., Solazzo, E., Guion, A., Muntean, M., Florczyk, A., Schiavina, M., Melchiorri, M., and Hutfilter, A. F.: Global anthropogenic emissions in urban areas: patterns, trends, and challenges, Environ. Res. Lett., 16, 074033, https://doi.org/10.1088/1748-9326/ac00e2, 2021.

Crippa, M., Guizzardi, D., Butler, T., Keating, T., Wu, R., Kaminski, J., Kuenen, J., Kurokawa, J., Chatani, S., Morikawa, T., Pouliot, G., Racine, J., Moran, M. D., Klimont, Z., Manseau, P. M.,

Mashayekhi, R., Henderson, B. H., Smith, S. J., Suchyta, H., Muntean, M., Solazzo, E., Banja, M., Schaaf, E., Pagani, F., Woo, J.-H., Kim, J., Monforti-Ferrario, F., Pisoni, E., Zhang, J., Niemi, D., Sassi, M., Ansari, T., and Foley, K.: HTAP_v3 emission mosaic: a global effort to tackle air quality issues by quantifying global anthropogenic air pollutant sources, Earth Syst. Sci. Data, 15, 2667–2694, https://doi.org/10.5194/essd-15-2667-2023, 2023.

Doumbia, T., Granier, C., Elguindi, N., Bouarar, I., Darras, S., Brasseur, G., Gaubert, B., Liu, Y., Shi, X., Stavrakou, T., Tilmes, S., Lacey, F., Deroubaix, A., and Wang, T.: Changes in global air pollutant emissions during the COVID-19 pandemic: a dataset for atmospheric modeling, Earth Syst. Sci. Data, 13, 4191–4206, https://doi.org/10.5194/essd-13-4191-2021, 2021.

Flemming, J., Huijnen, V., Arteta, J., Bechtold, P., Beljaars, A., Blechschmidt, A.-M., Diamantakis, M., Engelen, R. J., Gaudel, A., Inness, A., Jones, L., Josse, B., Katragkou, E., Marecal, V., Peuch, V.-H., Richter, A., Schultz, M. G., Stein, O., and Tsikerdekis, A.: Tropospheric chemistry in the Integrated Forecasting System of ECMWF, Geosci. Model Dev., 8, 975–1003, https://doi.org/10.5194/gmd-8-975-2015, 2015.

Ganguly, T., K. L. Selvaraj, S. K. Guttikunda, National Clean Air Programme (NCAP) for Indian cities: Review and outlook of clean air action plans, Atmos. Env., 8, https://doi.org/10.1016/j.aeaoa.2020.100096, 2020.

Gaubert, B., I. Bouarar, T. Doumbia, Y. Liu, T. Stavrakou, A. Deroubaix, S. Darras, N. Elguindi, C. Granier, F. Lacey, J. F. Muller, X. Shi, S. Tilmes, T. Wang, G. Brasseur, Global Changes in Secondary Atmospheric Pollutants During the 2020 COVID-19 Pandemic, J. Geophys. Res. Atmos., 126, https://doi.org/10.1029/2020JD034213, 2021.

Gaubert, B., D. P. Edwards, J. L. Anderson, A. F. Arellano, J. Barre, R. R., Buchholz, S. Darras, L. K. Emmons, D. Fillmore, C. Granier, J. W. Hannigan, I. Ortega, K. Raeder, A. Soulie, W. Tang, H. M. Worden, D. Ziskin, Global Scale Inversions from MOPITT CO and MODIS AOD, Remote Sensing, 15, https://doi.org/10.3390/rs15194813, 2023.

Granier, C., Bessagnet, B., Bond, T., A. D'Angiola, H. Denier van der Gon, G. J. Frost, A. Heil, J. W. Kaiser, S. Kinne, Z. Klimont, S. Kloster, J.-F. Lamarque, C. Liousse, T. Masui, F. Meleux, A. Mieville, T. Ohara, J.-C. Raut, K. Riahi, M. G. Schultz, S. J. Smith, A. Thompson, J. van Aardenne, G. R. van der Werf, D. van Vuuren, Evolution of anthropogenic and biomass burning emissions of air pollutants at global and regional scales during the 1980–2010 period, Climatic Change, 109, 163 https://doi.org/10.1007/s10584-011-0154-1, 2011.

Granier, C., C. Liousse, B. McDonald, P. Middleton, A. Soulie, S. Darras, M. Crippa, S. Dellaert, H. Denier van der Gon, T. Doumbia, M. Guevara, D. Guizzardi, C. Heyes, R. Hoesly, J.-P. Jalkanen, S. Keita, Z. Klimont, J. Kuenen, J. I. Kurokawa, M. Muntean, M. Osses, K. Sindelarova, S. Smith, Anthropogenic emissions inventories of air pollutants, In: Akimoto, H., Tanimoto, H. (eds) Handbook of Air Quality and Climate Change. Springer, Singapore. https://doi.org/10.1007/978-981-15-2760-9_5, 2023.

Guevara, M., Jorba, O., Tena, C., Denier van der Gon, H., Kuenen, J., Elguindi, N., Darras, S., Granier, C., and Pérez García-Pando, C.: Copernicus Atmosphere Monitoring Service TEMPOral profiles (CAMS-TEMPO): global and European emission temporal profile maps for atmospheric chemistry modelling, Earth Syst. Sci. Data, 13, 367–404, https://doi.org/10.5194/essd-13-367-2021, 2021.

Hoesly, R. M., Smith, S. J., Feng, L., Klimont, Z., Janssens-Maenhout, G., Pitkanen, T., Seibert, J. J., Vu, L., Andres, R. J., Bolt, R. M., Bond, T. C., Dawidowski, L., Kholod, N., Kurokawa, J.-I., Li, M., Liu, L.,

Lu, Z., Moura, M. C. P., O'Rourke, P. R., and Zhang, Q.: Historical (1750–2014) anthropogenic emissions of reactive gases and aerosols from the Community Emissions Data System (CEDS), Geosci. Model Dev., 11, 369–408, https://doi.org/10.5194/gmd-11-369-2018, 2018.

Huang, G., Brook, R., Crippa, M., Janssens-Maenhout, G., Schieberle, C., Dore, C., Guizzardi, D., Muntean, M., Schaaf, E., and Friedrich, R.: Speciation of anthropogenic emissions of non-methane volatile organic compounds: a global gridded data set for 1970–2012, Atmos. Chem. Phys., 17, 7683–7701, https://doi.org/10.5194/acp-17-7683-2017, 2017.

Inness, A., Ades, M., Agustí-Panareda, A., Barré, J., Benedictow, A., Blechschmidt, A.-M., Dominguez, J. J., Engelen, R., Eskes, H., Flemming, J., Huijnen, V., Jones, L., Kipling, Z., Massart, S., Parrington, M., Peuch, V.-H., Razinger, M., Remy, S., Schulz, M., and Suttie, M.: The CAMS reanalysis of atmospheric composition, Atmos. Chem. Phys., 19, 3515–3556, https://doi.org/10.5194/acp-19-3515-2019, 2019.

Jiang, Z., McDonald, B. C., Worden, H., Worden, J. R., Miyazaki, K., Qu, Z., Henze, D. K., Jones, D. B. A., Arellano, A. F., Fischer, E. V., Zhu, L., F. Boersma, Unexpected slowdown of US pollutant emission reduction in the past decade, Proc. Natl. Acad. Sci. U.S.A, 115, 5099-5104, https://doi.org/10.1073/pnas.1801191115, 2018.

Johansson, L., Jalkanen, J.-P., and Kukkonen, J. Global assessment of shipping emissions in 2015 on a high spatial and temporal resolution Atmospheric Environment 167, 403-415, https://doi.org/10.1016/j.atmosenv.2017.08.042, 2017.

Joshi, A., M. Pathak, J. Kuttippurath, V.K. Patel, Adoption of cleaner technologies and reduction in fire events in the hotspots lead to global decline in carbon monoxide, Chemosphere, 333, https://doi.org/10.1016/j.chemosphere.2023.139259, 2023.

Kuenen, J., Dellaert, S., Visschedijk, A., Jalkanen, J.-P., Super, I., and Denier van der Gon, H.: CAMS-REG-v4: a state-of-the-art high-resolution European emission inventory for air quality modelling, Earth Syst. Sci. Data, 14, 491–515, https://doi.org/10.5194/essd-14-491-2022, 2022.

Kurokawa, J. and Ohara, T.: Long-term historical trends in air pollutant emissions in Asia: Regional Emission inventory in ASia (REAS) version 3, Atmos. Chem. Phys., 20, 12761-12793, https://doi.org/10.5194/acp-20-12761-2020, 2020.

Li, M., Liu, H., Geng, G., Hong, C., Liu, F., Song, Y., Tong, D., Zheng, B., Cui, H., Man, H., Zhang, Q., and He, K.: Anthropogenic emission inventories in China: a review, Natl. Sci. Rev., 4, 834-866, doi: 10.1093/nsr/nwx150, 2017.

McDuffie, E. E., Smith, S. J., O'Rourke, P., Tibrewal, K., Venkataraman, C., Marais, E. A., Zheng, B., Crippa, M., Brauer, M., and Martin, R. V.: A global anthropogenic emission inventory of atmospheric pollutants from sector- and fuel-specific sources (1970–2017): an application of the Community Emissions Data System (CEDS), Earth Syst. Sci. Data, 12, 3413–3442, https://doi.org/10.5194/essd-12-3413-2020, 2020.

Miller, B. B. and Carter, C.: The test article, J. Sci. Res., 12, 135–147, doi:10.1234/56789, 2015.

Smith, A. A., Carter, C., and Miller, B. B.: More test articles, J. Adv. Res., 35, 13–28, doi:10.2345/67890, 2014.

O'Rourke, P. R, Smith, S. J., Mott, A., Ahsan, H., McDuffie, E. E., Crippa, M., Klimont, S., McDonald, B., Z., Wang, Nicholson, M. B, Feng, L., and Hoesly, R. M., Community Emissions Data System (Version 04-21-2021). Zenodo. https://doi.org/10.5281/zenodo.4737769, 2021a.

O'Rourke, P. R, Smith, S. J., Mott, A., Ahsan, H., McDuffie, E. E., Crippa, M., Klimont, S., McDonald, B., Z., Wang, Nicholson, M. B, Feng, L., and Hoesly, R. M., Community Emissions Data System Gridded Emissions (Version 04-21-2021). PNNL. https://doi.org/10.25584/PNNLDataHub/1779095, 2021b.

Ortega, I., B. Gaubert, J. W. Hannigan, G. Brasseur, H. M. Worden, T. Blumenstock, H. Fu, F. Hase, P. Jeseck, N. Jones, N., C. Liu, E. Mahieu, I. Morino, I. Murata, J. Notholt, M. Palm, A. Roehling, Y. Te, K. Strong, Y. Sun, S. Yamanouchi, Anomalies of O3, CO, C2,H2, H2CO, and C2H6 detected with multiple ground-based Fourier-transform infrared spectrometers and assessed with model simulation in 2020: COVID-19 lockdowns versus natural variability. Elem. Sci. Anth. 11, https://doi.org/10.1525/elementa.2023.00015, 2023.

Peuch, V.-H., R. Engelen, M. Rixen, D. Dee, J. Flemming, M. Suttie, M. Ades, A. Agusti-Panareda, C. Ananasso, E. Andersson, D. Armstrong, J. Barre, N. Bousserez, J. J. Dominguez, S. Garrigues, A., Inness, L. Jones, Kipling, J. Letertre-Danczak, M. Parrington, M. Razinger, R. Ribas, S. Vermoote, X. Yang, A. Simmons, J. Garces de Marcilla, The Copernicus Atmosphere Monitoring Service: from research to operations, Bull. Am. Met. Soc., 103, https://doi.org/10.1175/BAMS-D-21-0314.1, 2022.

Riahi, K., Rao, S., Krey, V., Cho, C., Chirkov, V., Fischer, G., Kindermann, G., Nakicenovic, N. and Rafaj, P., RCP 8.5 - A scenario of comparatively high greenhouse gas emissions. Climatic change, 109, 33-57, https://doi.org/10.1007/s10584-011-0149-y, 2011.

Soulie, A., C. Granier, S. Darras, N. Zilbermann, T. Doumbia, M. Guevara, J.-P. Jalkanen, S. Keita, C. Liousse, M. Crippa, D. Guizzardi, R. Hoesly, S. J. Smith, Global Anthropogenic Emissions (CAMS-GLOB-ANT) for the Copernicus Atmosphere Monitoring Service Simulations of Air Quality Forecasts and Reanalyses, https://doi.org/10.24380/eets-qd81, submitted to Earth Syst. Sci. Data, 2023.

Tang, W., Emmons, L. K., Worden, H. M., Kumar, R., He, C., Gaubert, B., Zheng, Z., Tilmes, S., Buchholz, R. R., Martinez-Alonso, S.-E., Granier, C., Soulie, A., McKain, K., Daube, B., Peischl, J., Thompson, C., and Levelt, P.: Application of the Multi-Scale Infrastructure for Chemistry and Aerosols version 0 (MUSICAv0) for air quality in Africa, Geosci. Model Dev. Discuss. [preprint], https://doi.org/10.5194/gmd-2023-50, in review, 2023.

Wankmüller, R.: Updated documentation of the EMEP gridding system, Technical Report CEIP 6/2019, available at: https://www.ceip.at/fileadmin/inhalte/ceip/00_pdf_other/2019/emep_gridding_system_documentation_20191125.pdf (last access: July 2023), 2019.

Zheng, B., Tong, D., Li, M., Liu, F., Hong, C., Geng, G., Li, H., Li, X., Peng, L., Qi, J., Yan, L., Zhang, Y., Zhao, H., Zheng, Y., He, K., and Zhang, Q.: Trends in China's anthropogenic emissions since 2010 as the consequence of clean air actions, Atmos. Chem. Phys., 18, 14095–14111, https://doi.org/10.5194/acp-18-14095-2018, 2018.

Tables

Table 1: Global totals emitted in Tg/yr for selected species and associated percentage changes. CO_2 (fossil) corresponds to the CO_2 species, excluding short cycle. The NO_x emissions are reported as NO (M=30.01 g/mol).

	2000	2003	2006	2009	2012	2015	2018	2021	2023	Change 2012-2000	Change 2023-2012
CO_2 (fossil)	2.53e4	2.72e4	3.04e4	3.13e4	3.47e4	3.55e4	3.59e4	3.63e4	3.67e4	+37%	+5.7%
CH_4	302	310	331	339	360	370	372	375	378	+19%	+5%
CO	556	528	526	537	564	578	562	550	542	+1.4%	-4%
NO_x	72.6	73.4	76.7	74.4	79.3	78.2	75.1	73.0	71.8	+9%	-10%
NMVOCs	122	125	132	133	143	149	147	146	145	+17%	+1%
SO_2	97.9	94.7	101	100	105	102	92.7	79.1	76.0	+7%	-28%
BC	3.8	3.91	4.16	4.47	4.79	4.68	4.56	4.45	4.40	+26%	-8%
OC	9.9	10	10.6	11.1	11.6	11.8	11.6	11.3	11.2	+17%	-3%
NH_3	40.9	42.5	44.4	46	47.7	49.1	49.6	50.2	50.6	+17%	+6%

Table 2: Totals emitted in Tg/yr and associated percentage changes for Western Europe. The values for the NO_x emissions are given in Tg NO_x (as NO)/yr.

	2000	2003	2006	2009	2012	2015	2018	2021	2023	Change 2012-2000	Change 2023-2012
CO_2 (fossil)	3.17e3	3.28e3	3.26e3	2.91e3	2.85e3	2.68e3	2.59e3	2.52e3	2.48e3	-9%	-13%
CH_4	21.8	20.7	20.4	18.3	18.6	18.4	18.3	18.2	18.2	-15%	-2%
CO	38.5	31.2	23.9	18.7	15.9	14.6	14.1	13.8	13.6	-58%	-14%
NO_x	6.4	6.0	5.3	4.5	4.0	3.7	3.4	3.1	3.0	-37%	-26%
NMVOCs	8.5	7.6	6.7	6.1	5.9	5.8	5.8	5.7	5.7	-31%	-3%
SO_2	4.9	3.9	3.3	2.6	2.5	2.2	1.9	1.7	1.6	-49%	-38%
BC	0.18	0.16	0.15	0.14	0.13	0.12	0.11	0.1	0.1	-29%	-22%
OC	0.27	0.26	0.25	0.26	0.25	0.25	0.24	0.23	0.23	-7%	-10%
NH_3	4.6	4.5	4.3	4.3	4.3	4.4	4.4	4.4	4.4	-7%	+3%

Table 3: Totals emitted in Tg/yr and associated percentage changes for Central Europe. CO_2_excl corresponds to the CO_2 species, excluding short cycle. The values for the NO_x emissions are given in Tg NO_x (as NO)/yr.

	2000	2003	2006	2009	2012	2015	2018	2021	2023	Change 2012-2000	Change 2023-2012
CO_2 (fossil)	843	886	908	825	829	793	801	816	819	-1.7%	-1.2%
CH_4	7.7	6.5	6.5	6.2	6.4	6.3	6.3	6.3	6.3	-17%	-2%
CO	9.2	8.8	8.9	7.8	7.4	7.1	7	6.8	6.8	-20%	-8%
NO_x	1.6	1.6	1.6	1.4	1.3	1.2	1.1	1.1	1.0	-19%	-19%
NMVOCs	2.7	2.7	2.7	2.5	2.4	2.4	2.4	2.4	2.4	-9%	0%
SO_2	4.2	3.9	3.2	2.8	2.8	2.6	2.0	1.7	1.6	-33%	-43%
BC	0.06	0.063	0.067	0.070	0.74	0.072	0.070	0.068	0.068	+23%	-8%
OC	0.18	0.18	0.20	0.21	0.22	0.22	0.21	0.21	0.21	+21%	-5%
NH_3	1.3	1.3	1.3	1.3	1.3	1.4	1.4	1.4	1.4	+2%	+7%

Table 4: Totals emitted in Tg/yr and associated percentage changes for the USA. CO_2_excl corresponds to the CO_2 species, excluding short cycle. The values for the NO_x emissions are given in Tg NO_x (as NO)/yr.

	2000	2003	2006	2009	2012	2015	2018	2021	2023	Change 2012-2000	Change 2023-2012
CO_2 (fossil)	5.6e3	5.5e3	5.5e3	5.0e3	5.0e3	4.9e3	4.9e3	4.8e3	4.8e3	-11%	-4%
CH_4	23.9	22.4	22.4	22.5	23.9	25.1	25.3	25.5		0%	+7%
CO	85.6	68.1	54.2	46.1	45.4	45.7	42.3	39.3	37.4	-47%	-18%
NO_x	10.9	10.2	9.5	8.1	8.3	8.4	7.4	6.6	6.3	-24%	-24%
NMVOCs	12.2	11.1	10.7	9.9	9.9	10.2	9.6	9.1	8.8	-18%	-12%
SO_2	13.7	12.0	10.9	9.7	8.9	8.1	5.9	4.4	3.6	-35%	-59%
BC	0.22	0.21	0.21	0.16	0.17	0.17	0.16	0.15	0.14	-19%	-19%
OC	0.39	0.35	0.35	0.33	0.33	0.34	0.32	0.3	0.3	-14%	-12%
NH_3	3.6	3.8	3.9	3.8	3.9	3.9	4.0	4.1	4.2	+9%	+8%

Table 5: Totals emitted in Tg/yr and associated percentage changes for China. CO_2_excl corresponds to the CO_2 species, excluding short cycle. The values for the NO_x emissions are given in Tg NO_x (as NO)/yr.

	2000	2003	2006	2009	2012	2015	2018	2021	2023	Change 2012-2000	Change 2023-2012
CO_2 (fossil)	3.5e3	4.5e3	6.6e3	7.9e3	9.7e3	1.0e4	1.0e4	1.1e4	1.1e4	+180%	+14%
CH_4	44.6	46.1	53.2	55.7	59.5	60.6	61.3	62.1	62.6	+33%	+5%
CO	101	99	113	115	124	125	120	114	111	+23%	-10%
NO_x	8.3	10.0	13.6	14.5	15.7	15.9	14.6	14.2	14.0	+90%	-11%
NMVOCs	18.9	20.4	23.9	26.0	28.4	30.1	29.7	29.4	29.2	+50%	+3%
SO_2	19.6	21.4	28.0	29.3	30.5	29.1	23.0	18.5	16.1	+56%	-47%
BC	0.0	1.0	1.1	1.3	1.4	1.2	1.2	1.1	1.1	+54%	-25%
OC	2.4	2.4	2.7	2.7	2.7	2.6	2.4	2.2	2.1	+21%	-22%
NH_3	8.2	8.4	8.8	8.8	8.6	8.6	8.7	8.7	8.7	+4%	+1%

Table 6: Totals emitted in Tg/yr and associated percentage changes for India. CO_2_excl corresponds to the CO_2 species, excluding short cycle. The values for the NO_x emissions are given in Tg NO_x (as NO)/yr.

	2000	2003	2006	2009	2012	2015	2018	2021	2023	Change 2012-2000	Change 2023-2012
CO_2 (fossil)	963	1.0e3	1.2e3	1.6e3	1.9e3	2.2e3	2.3e3	2.4e3	2.5e3	+99%	+32%
CH_4	27.3	28.0	29.7	31.0	32.4	33.2	33.5	33.7	33.9	+19%	+5%
CO	48	49	53	58	64	69	67	64	63	+34%	-10%
NO_x	3.3	3.4	3.9	4.9	5.8	6.6	6.6	6.6	6.6	+79%	+13%
NMVOCs	8.9	9.4	10.1	11.1	12.2	13.3	13.1	12.9	12.8	+37%	+5%
SO_2	4.9	5.1	5.8	7.9	9.9	11.2	11.2	11.2	11.2	+103%	+13%
BC	0.51	0.51	0.56	0.62	0.73	0.78	0.74	0.71	0.71	+43%	-6%
OC	1.4	1.4	1.4	1.6	1.7	1.8	1.8	1.7	1.7	+26%	-0.6%
NH_3	4.3	4.4	4.9	5.3	5.6	5.8	5.8	5.9	6.0	+32%	+6%

Figures

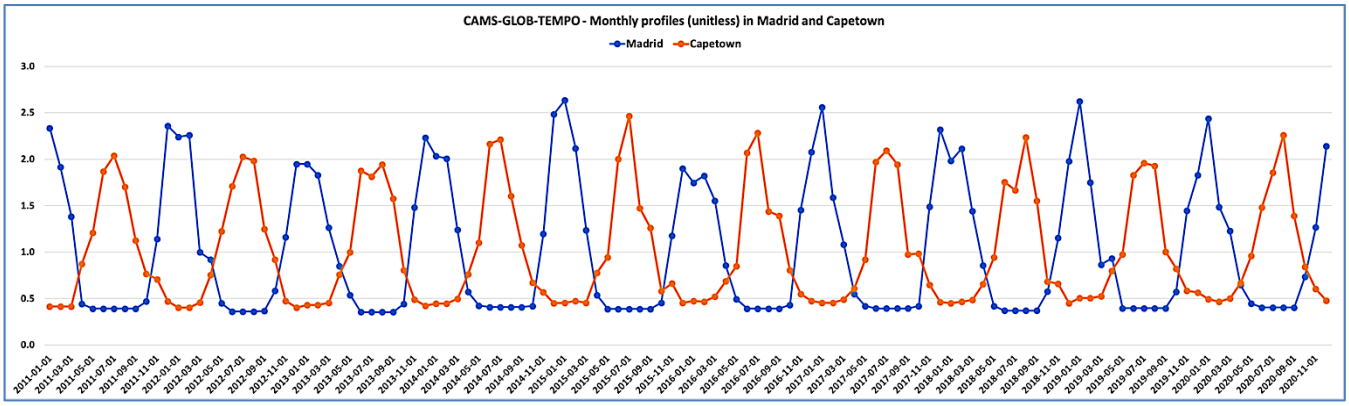

Figure 1: monthly weights from CAMS-GLOB-TEMPO in Madrid (Spain) and Capetown (South Africa) for the residential sector.

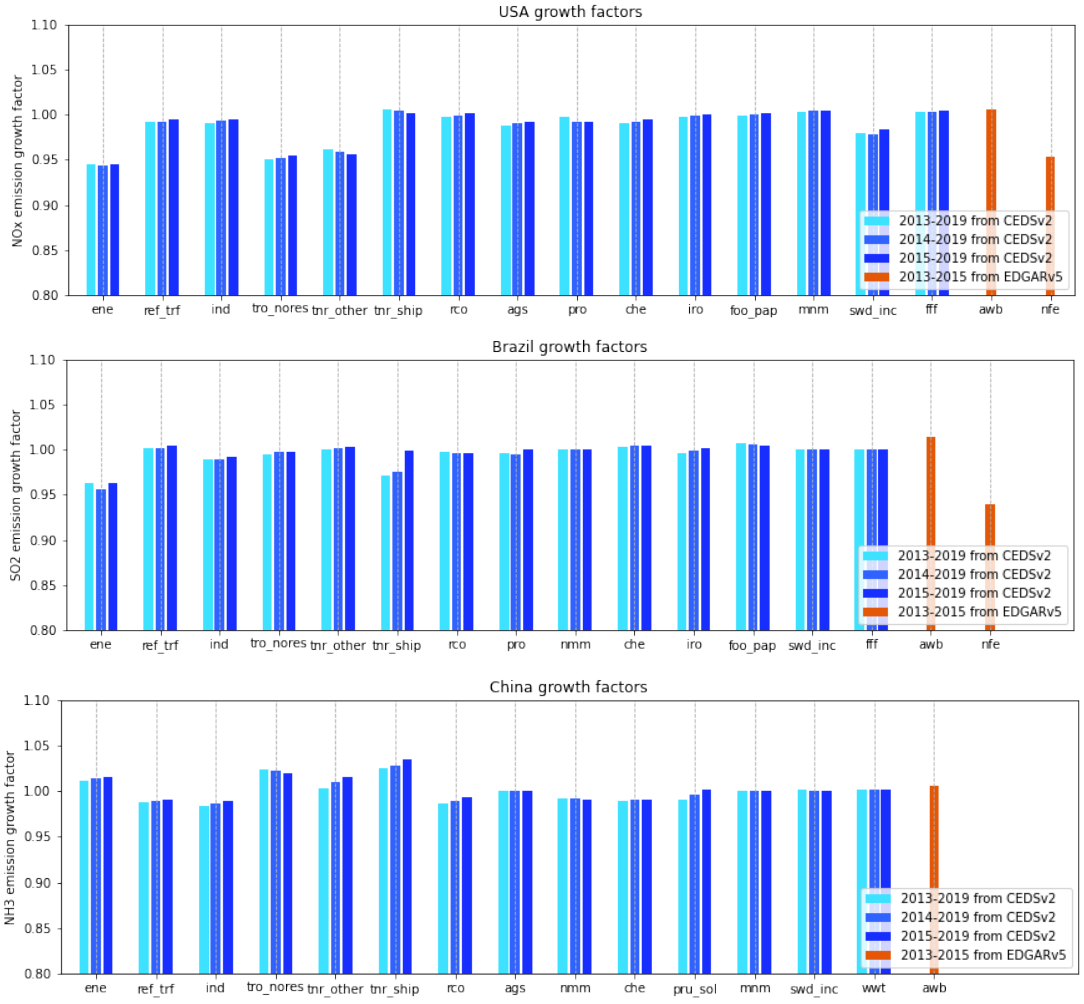

Figure 2: Relative changes in the emissions in the USA (top), Brazil (middle) and China (bottom) for different periods and different sectors

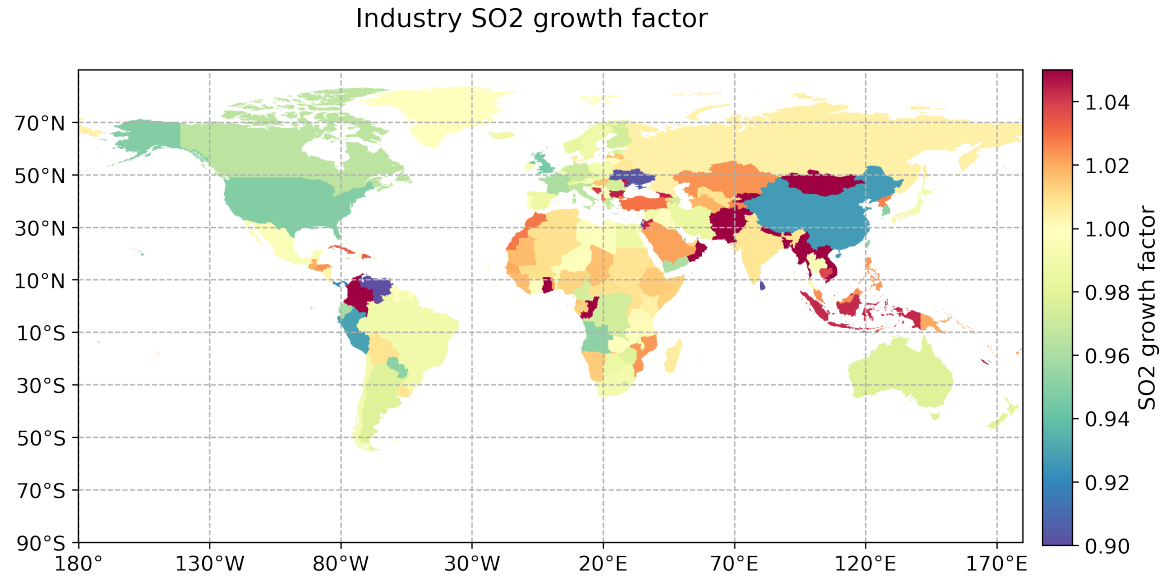

Figure 3: Growth factor for the industry sector used to extrapolate the SO_2 emissions

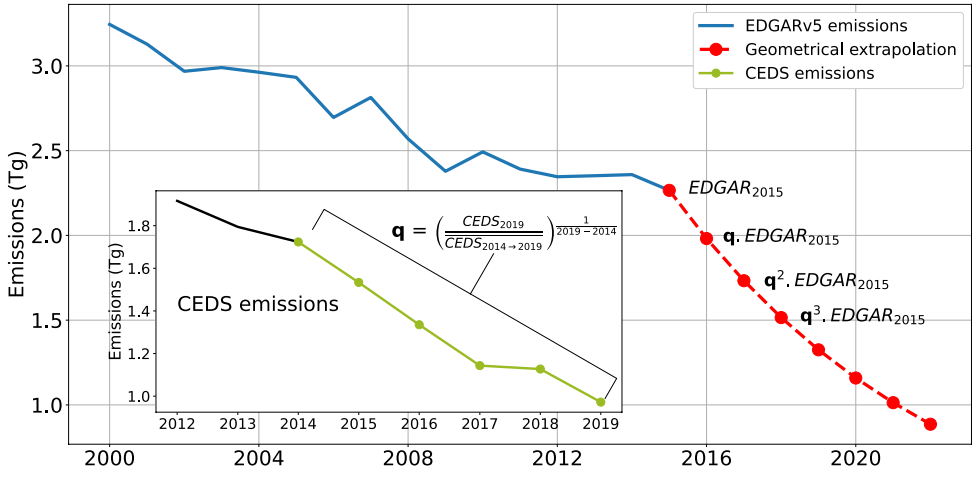

Figure 4: schematic view of the methodology used to calculate the CAMS-GLOB-ANT emissions for the most recent years.

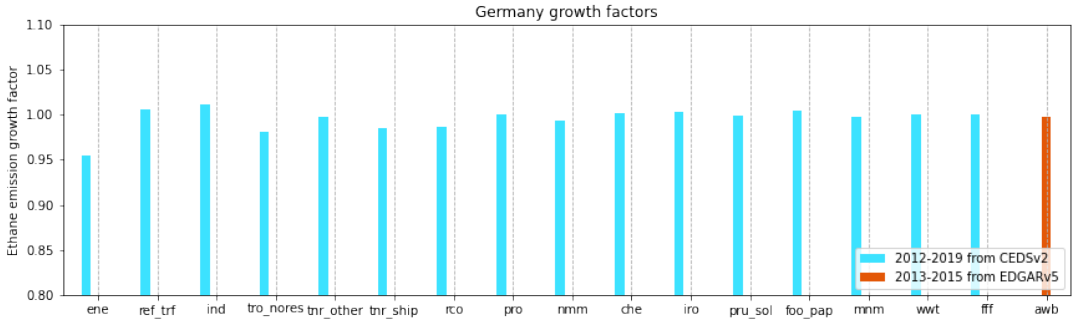

Figure 5: growth factor for the NMVOCs species for Germany

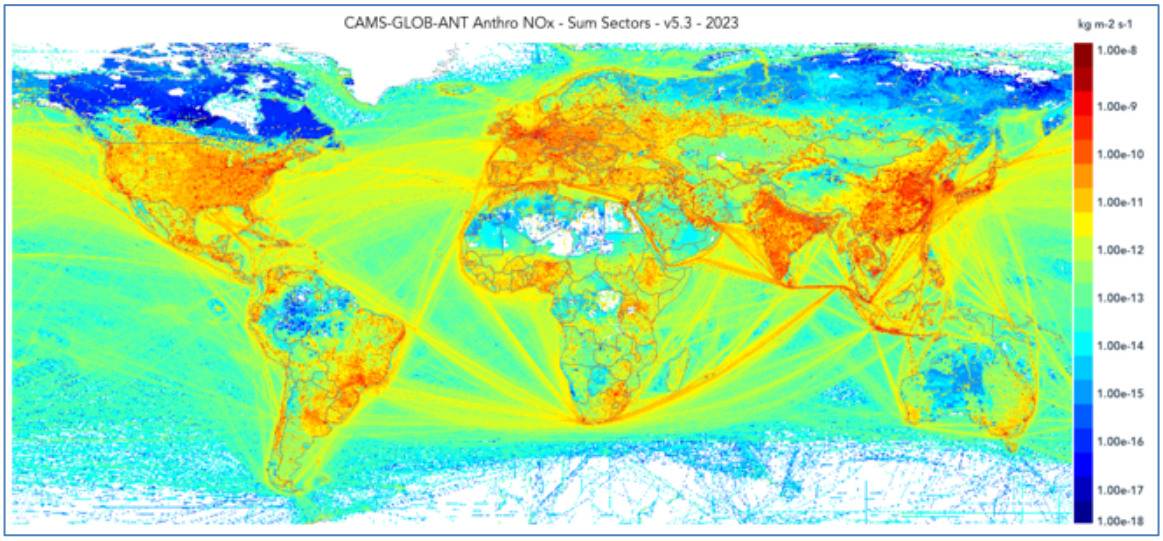
CAMS-GLOB-ANT Anthro NOx - Sum Sectors - v5.3 - 2023
kg m-2 s-1
1.00e-8
1.00e-9
1.00e-10
1.00e-11
1.00e-12
1.00e-13
1.00e-14
1.00e-15
1.00e-16
1.00e-17
1.00e-18

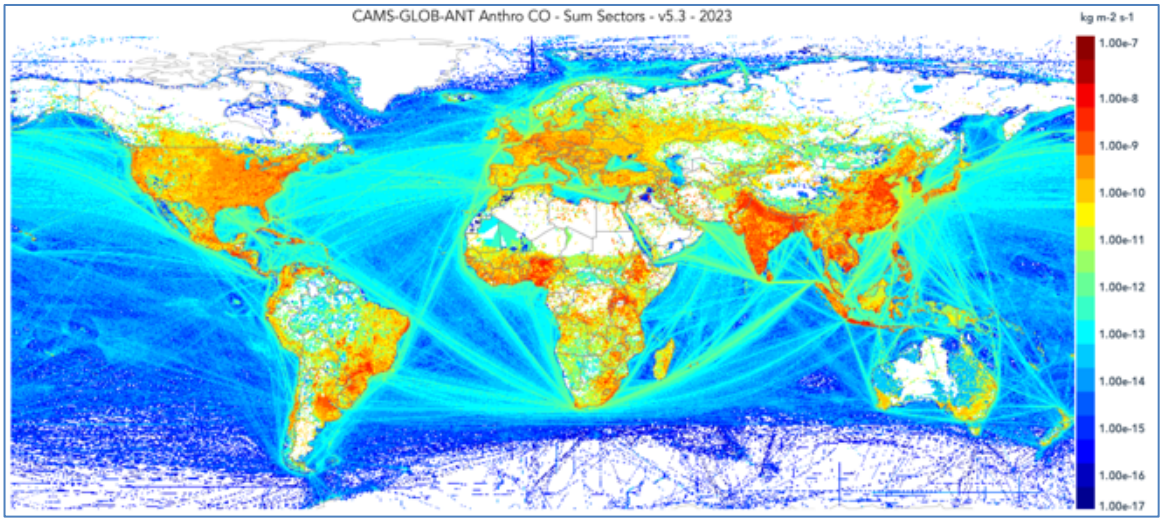
CAMS-GLOB-ANT Anthro CO - Sum Sectors - v5.3 - 2023
kg m-2 s-1
1.00e-7
1.00e-8
1.00e-9
1.00e-10
1.00e-11
1.00e-12
1.00e-13
1.00e-14
1.00e-15
1.00e-16
1.00e-17

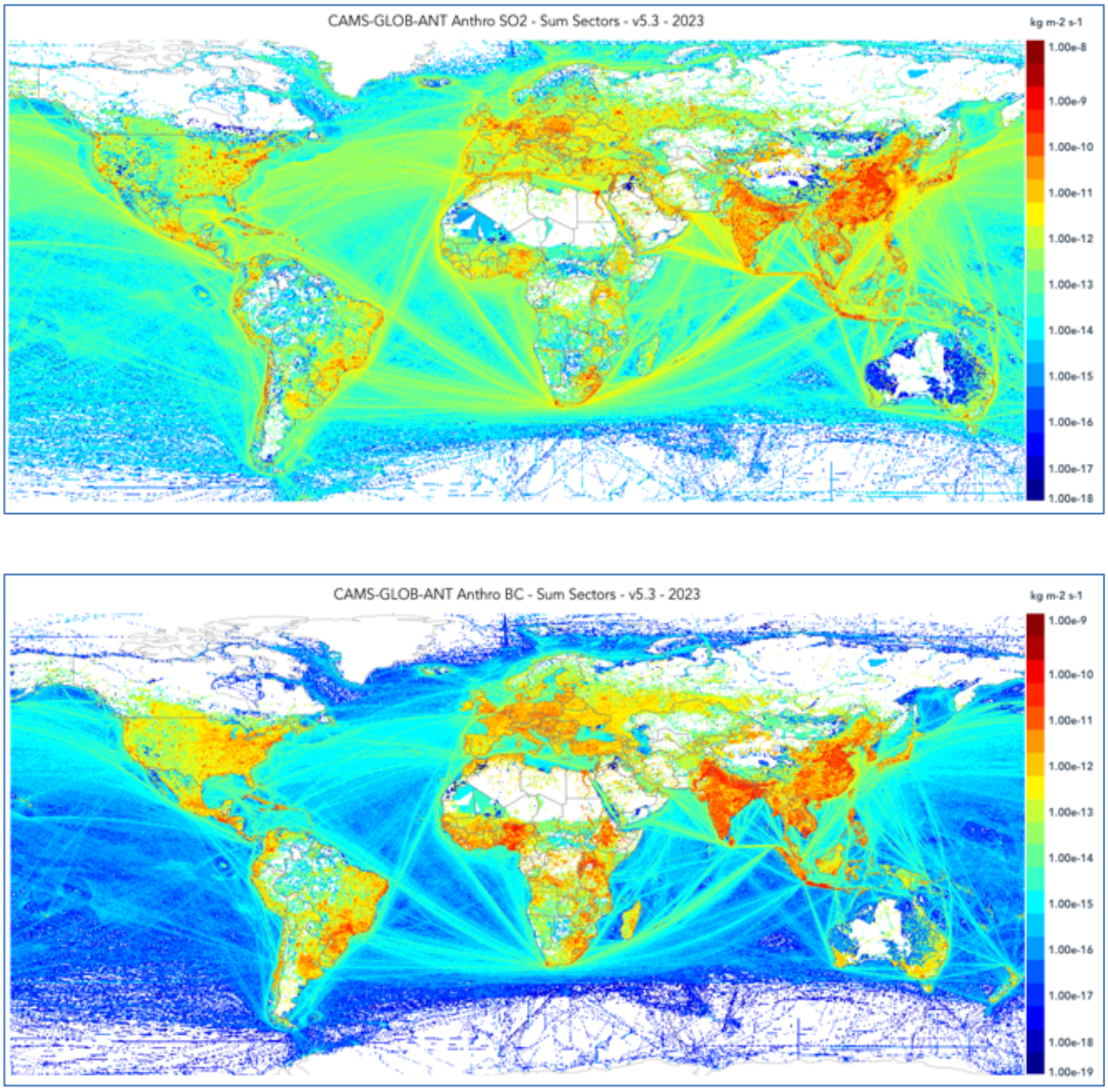

Figure 6: 2023 annual average of the surface emissions of NO_x (top left), CO (2nd from top), SO_2 (3rd from top) and BC (bottom), in kg/m2/s.

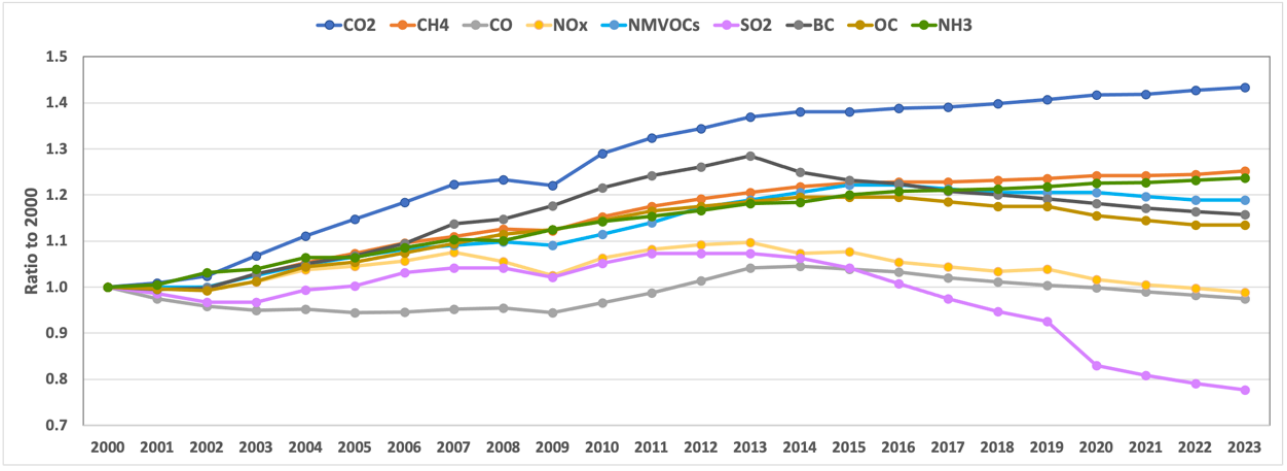

Figure 7: Relative change from 2000 in the global total emission of several species

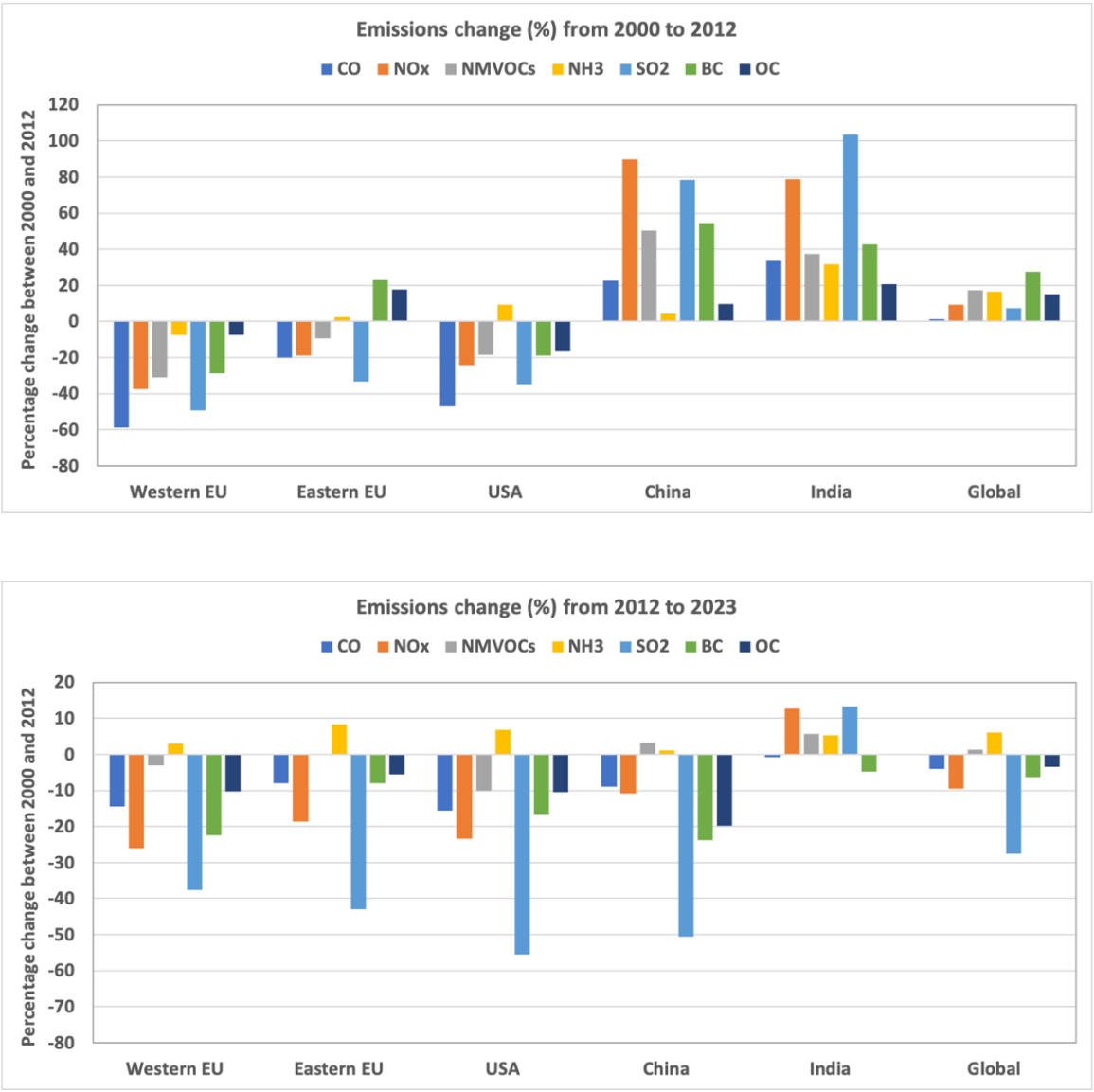

Figure 8: percentage change in the emissions of CO, NO_x, NMVOCs, NH_3, SO_2, BC and CO from 2000 to 2012 (top) and 2012 to 2023 (bottom).

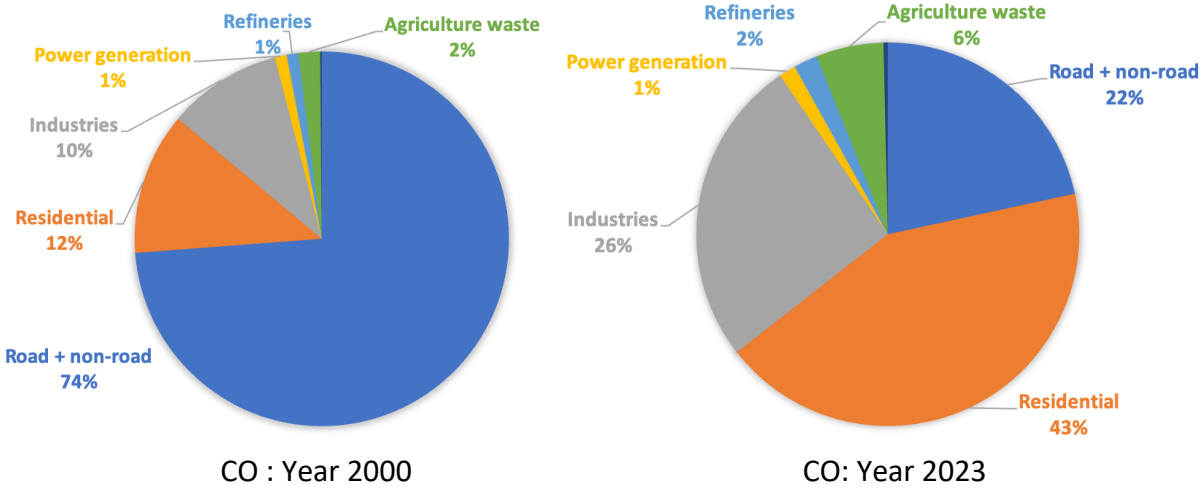

Figure 9: contribution of several sectors to the CO emissions in Western Europe in 2000 and 2023. The totals emitted for this region are 38.5 and 13.5 Tg/year in 2000 and 2023, respectively.

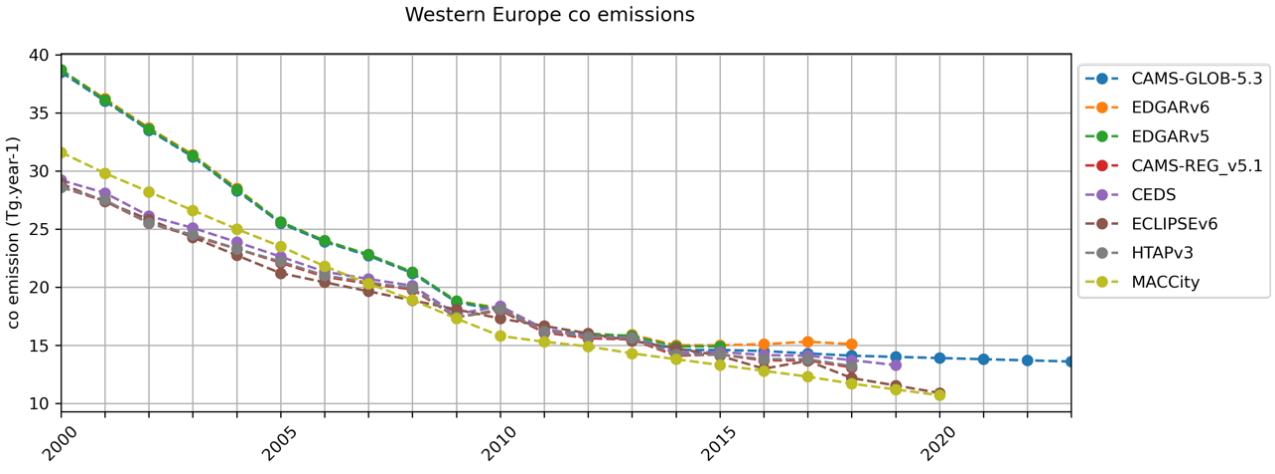
Western Europe co emissions
co emission (Tg.year-1)
40
35
30
25
20
15
10
2000
2005
2010
2015
2020
CAMS-GLOB-5.3
EDGARv6
EDGARv5
CAMS-REG_v5.1
CEDS
ECLIPSEv6
HTAPv3
MACCity

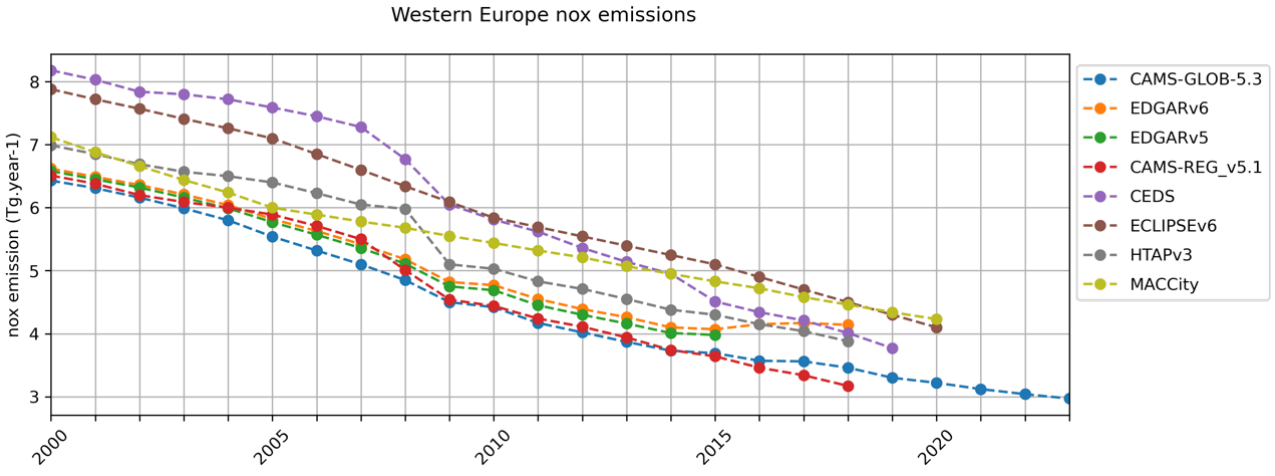
Western Europe nox emissions
nox emission (Tg.year-1)
8
7
6
5
4
3
2000
2005
2010
2015
2020
CAMS-GLOB-5.3
EDGARv6
EDGARv5
CAMS-REG_v5.1
CEDS
ECLIPSEv6
HTAPv3
MACCity

825

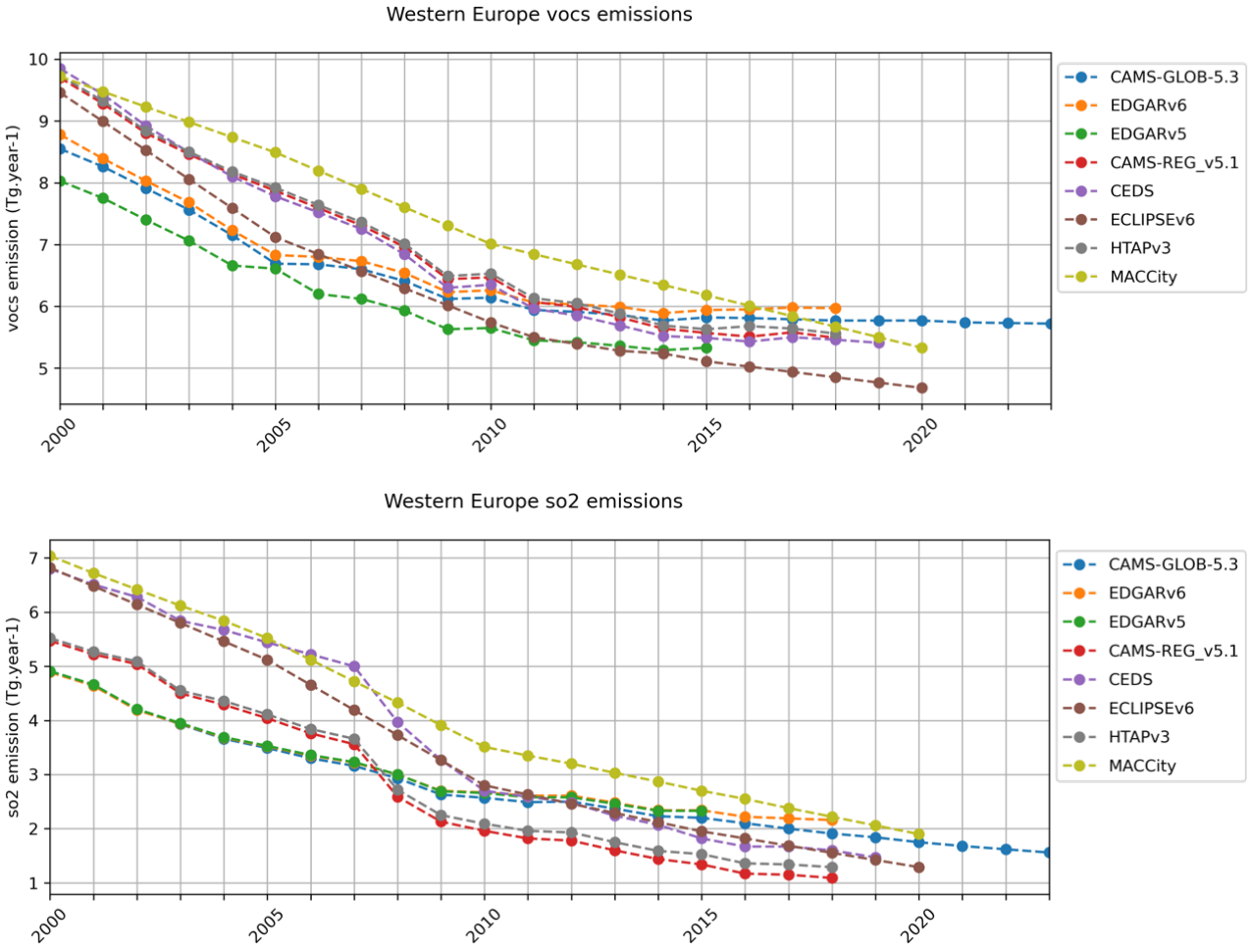

Figure 10: comparisons of the CAMS-GLOB-ANT_v5.3 emissions for CO, NO_x, NMVOCs and SO_2 with other global datasets and the CAMS-REG_V5.1 inventory.

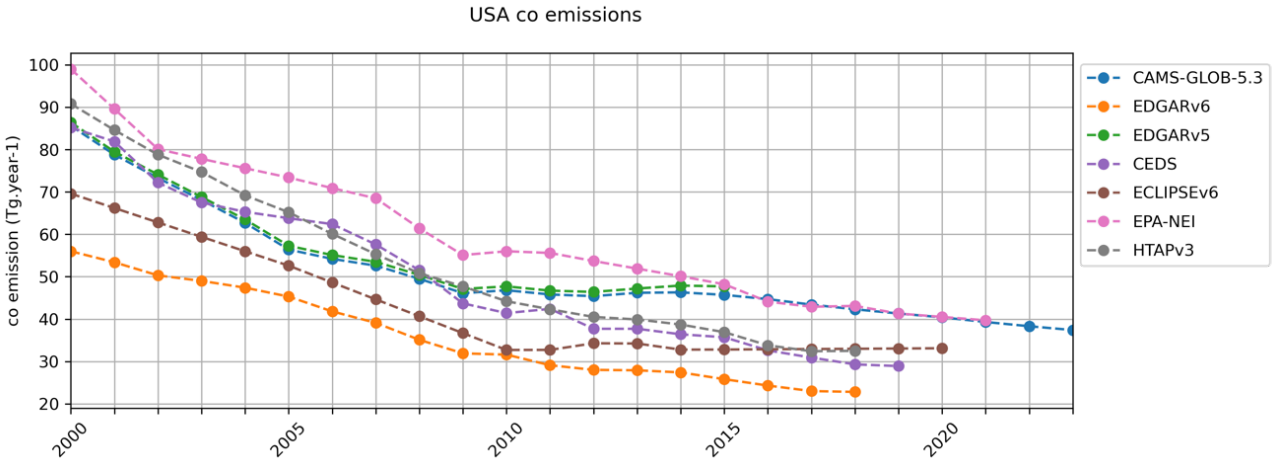
USA co emissions
co emission (Tg.year-1)
100
90
80
70
60
50
40
30
20
2000
2005
2010
2015
2020
CAMS-GLOB-5.3
EDGARv6
EDGARv5
CEDS
ECLIPSEv6
EPA-NEI
HTAPv3

835

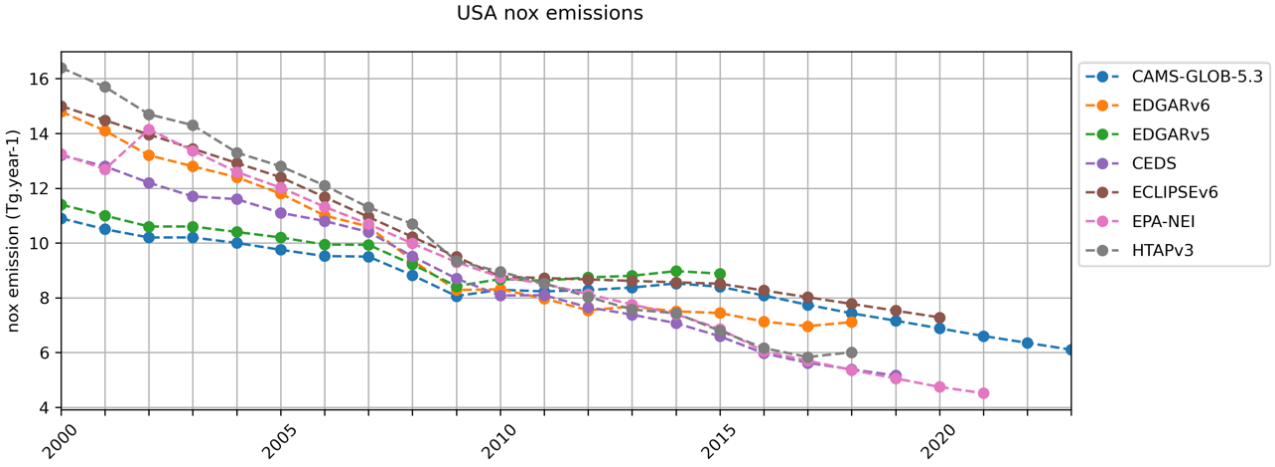
USA nox emissions
nox emission (Tg.year-1)
16
14
12
10
8
6
4
2000
2005
2010
2015
2020
CAMS-GLOB-5.3
EDGARv6
EDGARv5
CEDS
ECLIPSEv6
EPA-NEI
HTAPv3

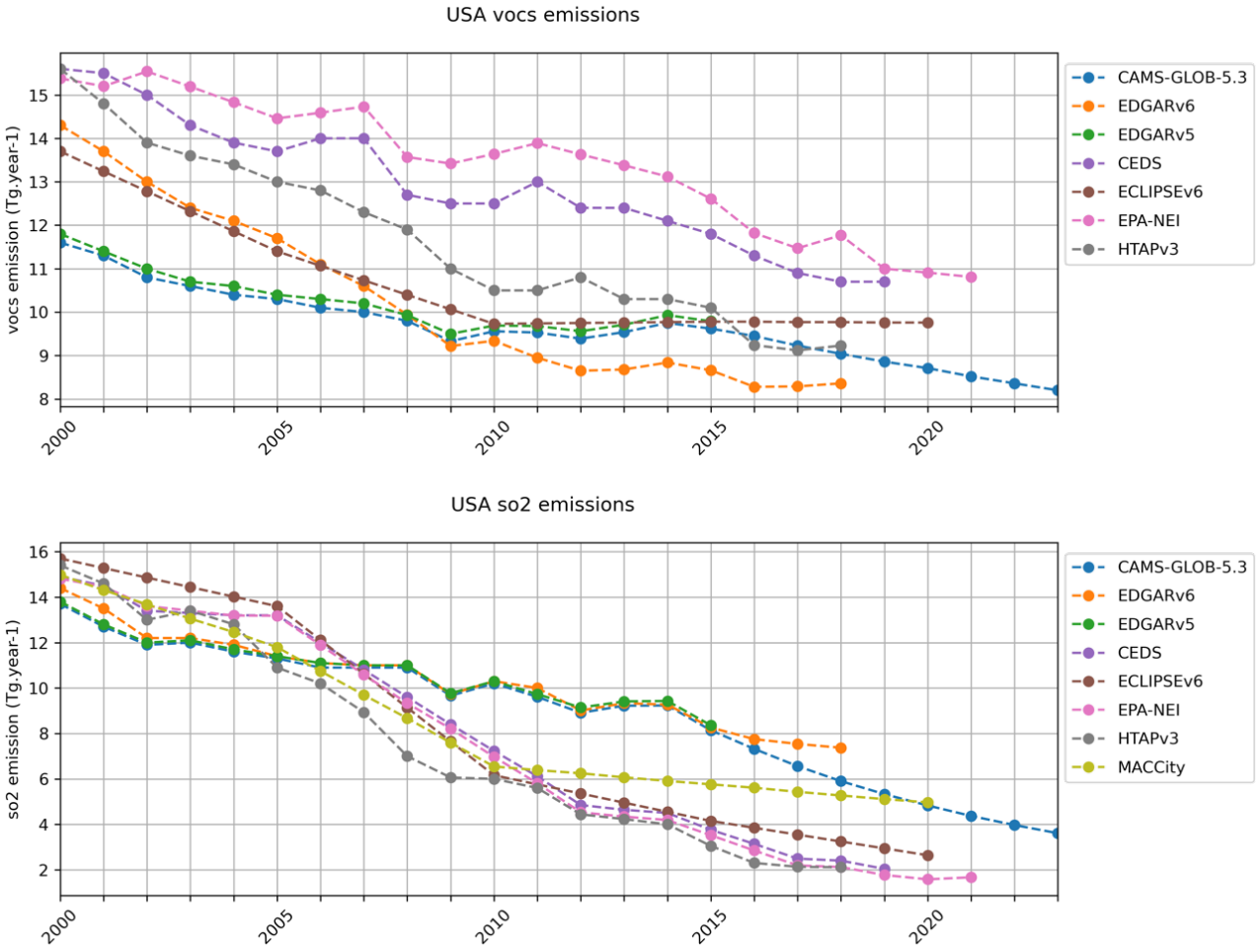

Figure 11: comparisons of the CAMS-GLOB-ANT_v5.3 emissions for CO, NO_x, NMVOCs and SO_2 with other global datasets and the EPA inventory.

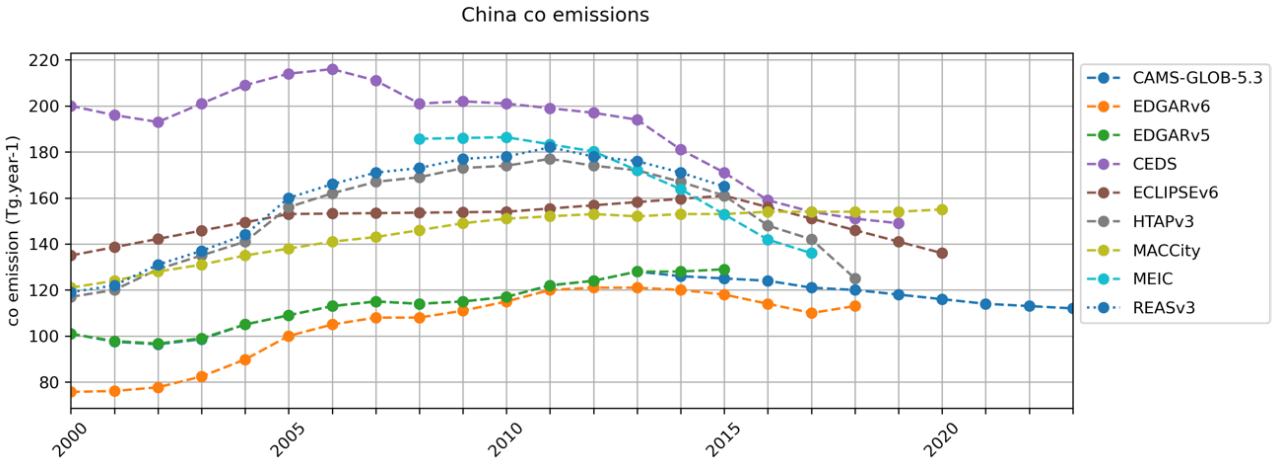
China co emissions
co emission (Tg.year-1)
220
200
180
160
140
120
100
80
2000
2005
2010
2015
2020
CAMS-GLOB-5.3
EDGARv6
EDGARv5
CEDS
ECLIPSEv6
HTAPv3
MACCity
MEIC
REASv3

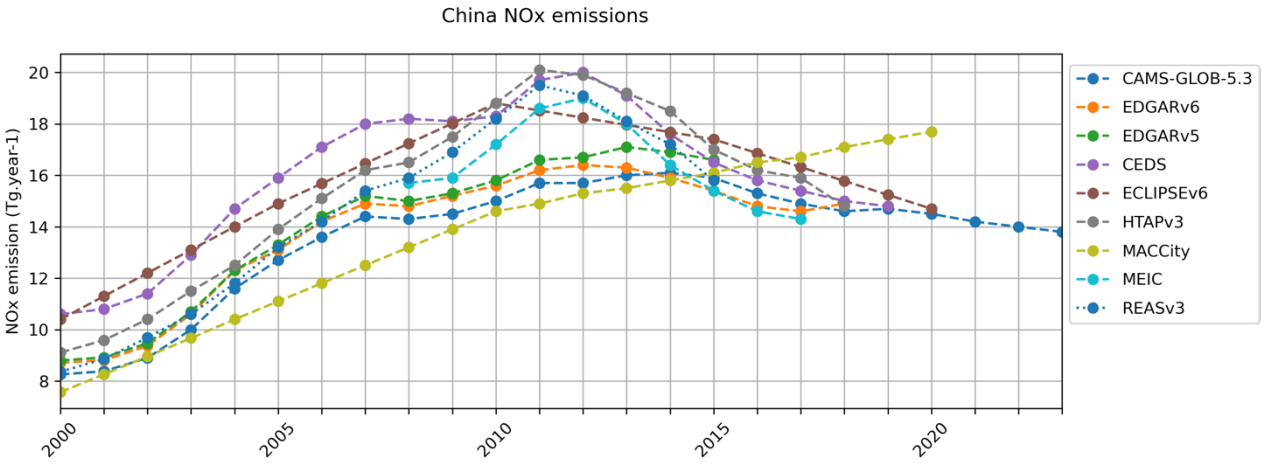
China NOx emissions
NOx emission (Tg.year-1)
20
18
16
14
12
10
8
2000
2005
2010
2015
2020
CAMS-GLOB-5.3
EDGARv6
EDGARv5
CEDS
ECLIPSEv6
HTAPv3
MACCity
MEIC
REASv3

845

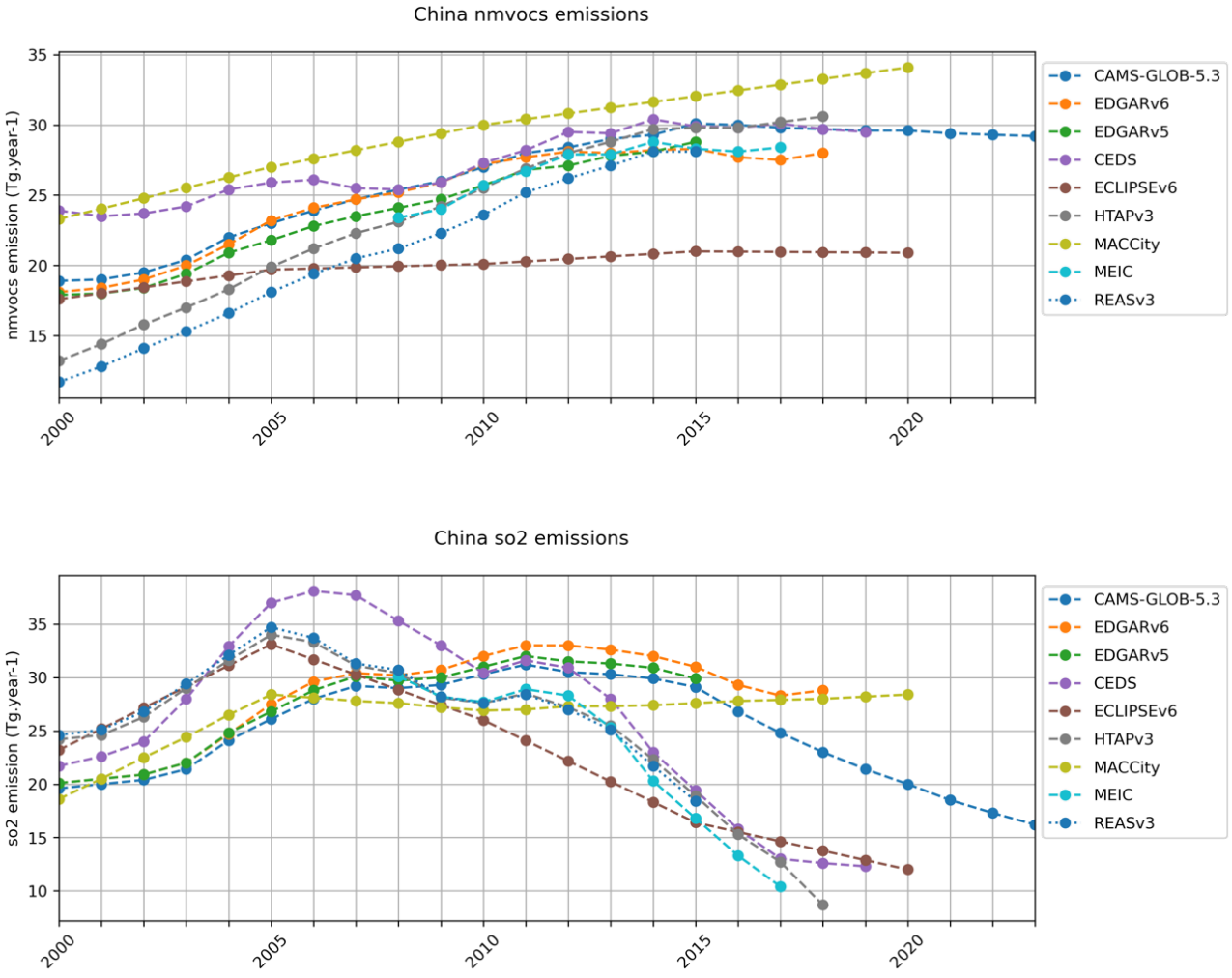

Figure 12: comparisons of the CAMS-GLOB-ANT_v5.3 emissions for CO, NO_x, NMVOCs and SO_2 with other global datasets and two regional inventories for China

855

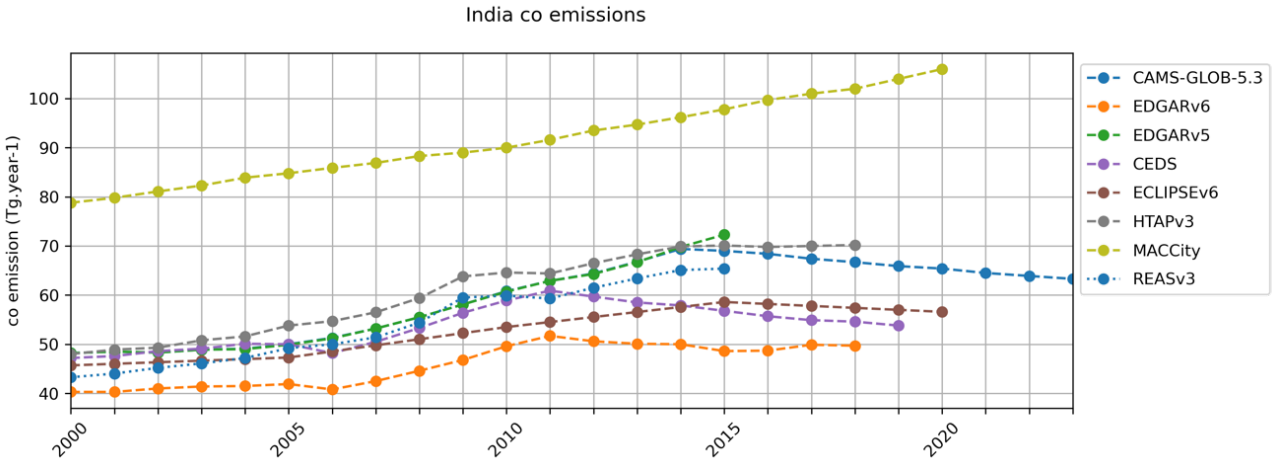
India co emissions
co emission (Tg.year-1)
100
90
80
70
60
50
40
2000
2005
2010
2015
2020
CAMS-GLOB-5.3
EDGARv6
EDGARv5
CEDS
ECLIPSEv6
HTAPv3
MACCity
REASv3

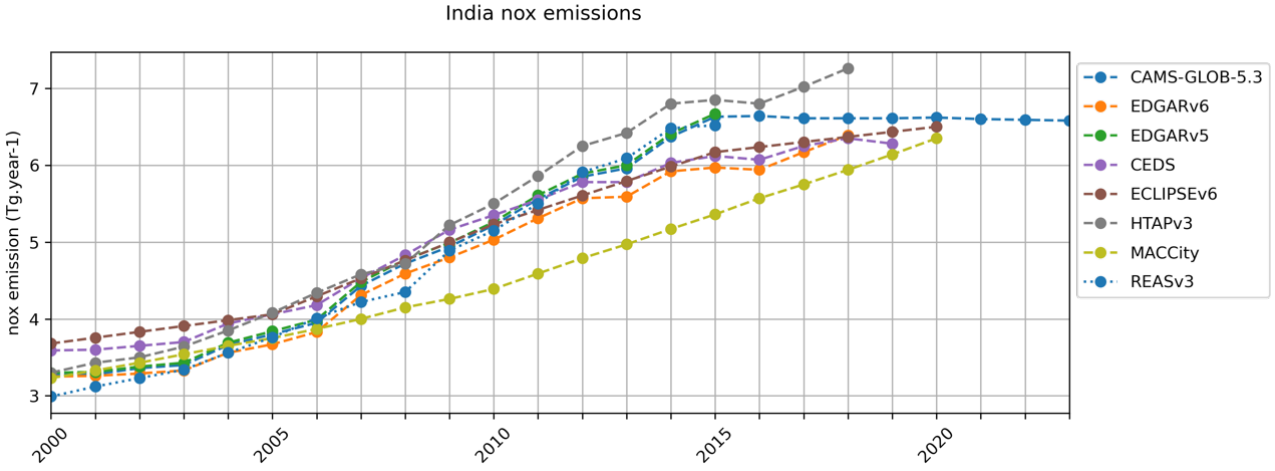
India nox emissions
nox emission (Tg.year-1)
7
6
5
4
3
2000
2005
2010
2015
2020
CAMS-GLOB-5.3
EDGARv6
EDGARv5
CEDS
ECLIPSEv6
HTAPv3
MACCity
REASv3

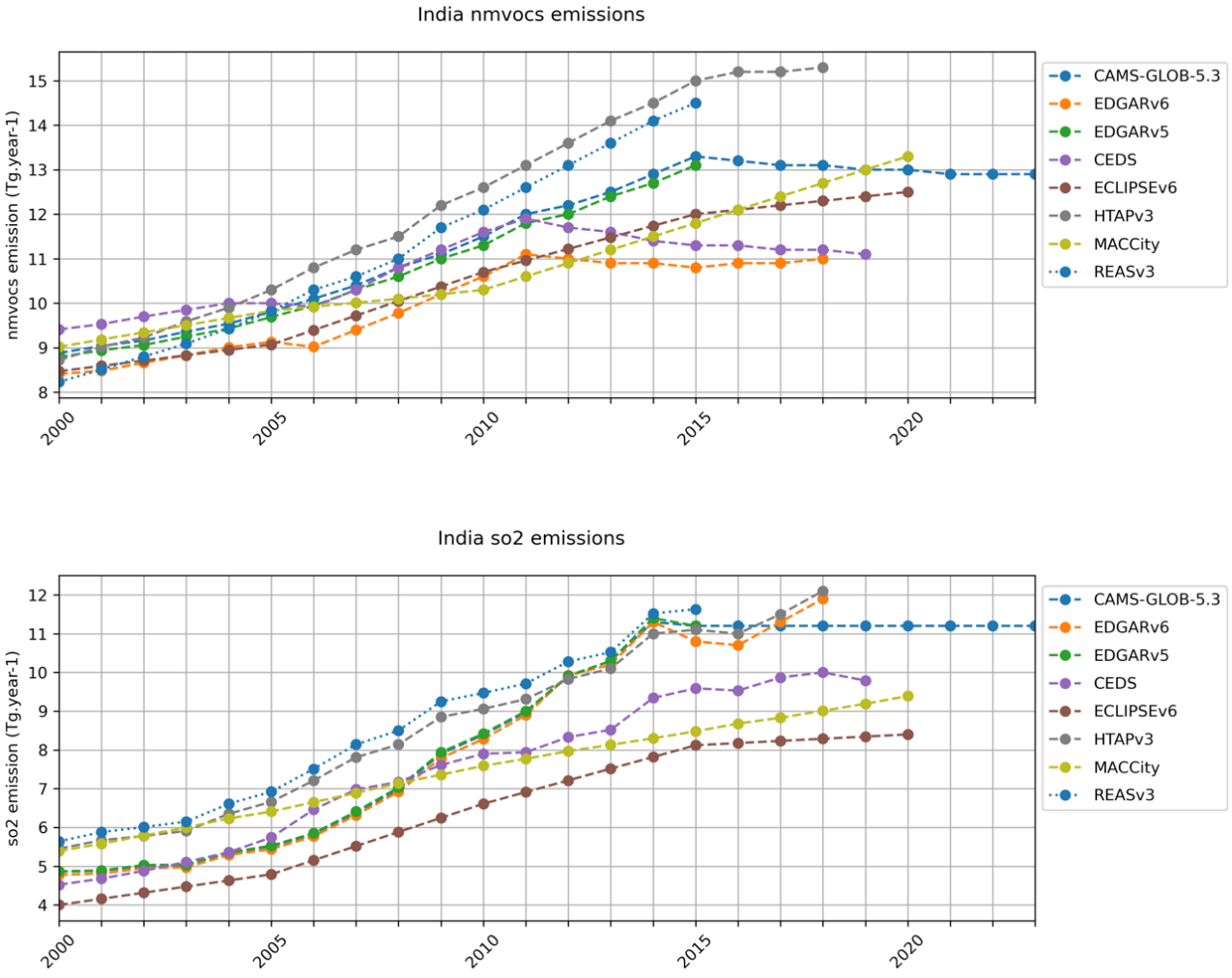

Figure 13: comparisons of the CAMS-GLOB-ANT_v5.3 emissions for CO, NO_x, NMVOCs and SO_2 with other global datasets and two regional inventories for India.